


# A Tomato Tocopherol-Binding Protein Sheds Light on Intracellular $\alpha$ -Tocopherol Metabolism in Plants

Luisa Bermúdez<sup>1</sup>, Talía del Pozo<sup>2</sup>, Bruno Silvestre Lira<sup>3</sup>, Fabiana de Godoy<sup>3</sup>, Irene Boos<sup>4</sup>, Cecilia Romanò<sup>4</sup>, Viola Previtali<sup>4</sup>, Juliana Almeida<sup>3,13</sup>, Claire Bréhélin<sup>5</sup>, Ramón Asis<sup>6</sup>, Leandro Quadrana<sup>1,14</sup>, Diego Demarco<sup>3</sup>, Saleh Alseekh<sup>7</sup>, Rigel Salinas Gamboa<sup>8</sup>, Laura Pérez-Flores<sup>8</sup>, Pia Guadalupe Dominguez<sup>1,15</sup>, Christophe Rothan <sup>9</sup>, Alisdair Robert Fernie<sup>7</sup>, Maurício González<sup>10</sup>, Achim Stocker<sup>11</sup>, Andreas Hemmerle<sup>11</sup>, Mads Hartving Clausen<sup>4</sup>, Fernando Carrari<sup>1,3,12,\*</sup> and Magdalena Rossi<sup>3,12,\*</sup>

<sup>1</sup>Instituto de Biotecnología, Instituto Nacional de Tecnología Agropecuaria (IB-INTA), and Consejo Nacional de Investigaciones Científicas y Técnicas (CONICET), PO Box 25, B1686WAA Castelar, Argentina

<sup>2</sup>Centro de Conservación y Propagación Vegetal (CEPROVEG), Facultad de Ciencias, Universidad Mayor, Santiago, Chile

<sup>3</sup>Departamento de Botânica, Instituto de Biociências, Universidade de São Paulo, Rua do Matão, 277, São Paulo, 05508-090, Brazil

<sup>4</sup>Center for Nanomedicine and Theranostics, Department of Chemistry, Technical University of Denmark, Kemitorvet 207, 2800, Kgs. Lyngby, Denmark

<sup>5</sup>CNRS, Laboratory of Membrane Biogenesis, UMR 5200, 33140 Villenave d'Ornon Cedex, France

<sup>6</sup>CIBICI, Facultad de Ciencias Químicas, Universidad Nacional de Córdoba, CC 5000, Córdoba, Argentina

<sup>7</sup>Max Planck Institute of Molecular Plant Physiology, Wissenschaftspark Golm, Am Mühlenberg 1, Potsdam-Golm, D-14476, Germany

<sup>8</sup>Laboratório de Fisiologia, Bioquímica y Biología Molecular de Plantas, Departamento de Ciencias de la Salud DCBS, Universidad Autónoma Metropolitana, 09340 Iztapalapa, Mexico, DF, Mexico

<sup>9</sup>INRA-Bordeaux, Fruit Biology and Pathology Unit, F-33883 Villenave d'Ornon, France

<sup>10</sup>Laboratório de Genética Molecular Vegetal, Universidad de Chile, Macul 13 5540, Santiago de Chile, Chile

<sup>11</sup>Department of Chemistry and Biochemistry, University of Berne, Freiestrasse 3, 3012 Berne, Switzerland

<sup>12</sup>These authors contributed equally to this work.

<sup>13</sup>Present address: School of Biological Sciences, Royal Holloway University of London, Egham, Surrey TW20 0EX, UK.

<sup>14</sup>Present address: Institut de Biologie de L'Ecole Normale Supérieure, Centre National de la Recherche Scientifique, Institut National de la Santé et de la Recherche Médicale, Ecole Normale Supérieure, Paris, France.

<sup>15</sup>Present address: Department of Forest Genetics and Plant Physiology, Umeå Plant Science Center, Umeå, Sweden.

\*Corresponding authors: Magdalena Rossi, E-mail, mrossi@usp.br; Fax, + 5511 3091 7556; Fernando Carrari,

E-mail, carrari.fernando@inta.gob.ar; Fax, +54 11 4621 1676.

(Received August 12, 2018; Accepted September 12, 2018)

**Tocopherols are non-polar compounds synthesized in the plastids, which function as major antioxidants of the plant cells and are essential in the human diet. Both the intermediates and final products of the tocopherol biosynthetic pathway must cross plastid membranes to reach their sites of action. So far, no protein with tocopherol binding activity has been reported in plants. Here, we demonstrated that the tomato SITBP protein is targeted to chloroplasts and able to bind  $\alpha$ -tocopherol. SITBP-knockdown tomato plants exhibited reduced levels of tocopherol in both leaves and fruits. Several tocopherol deficiency phenotypes were apparent in the transgenic lines, such as alterations in photosynthetic parameters, dramatic distortion of thylakoid membranes and significant variations in the lipid profile. These results, along with the altered expression of genes related to photosynthesis, and tetrapyrrole, lipid, isoprenoid, inositol/phosphoinositide and redox metabolism, suggest that SITBP may act in conducting tocopherol (or its biosynthetic intermediates) between the plastid compartments and/or at the interface between chloroplast and endoplasmic reticulum membranes, affecting interorganellar lipid metabolism.**

## Introduction

Tocopherols are non-polar compounds synthesized in the plastids of photosynthetic organisms. They are important lipid-soluble antioxidants that function as major photosynthetic activity protectants by scavenging singlet oxygen ( $^1O_2$ ) and reducing the extent of lipid peroxidation (Miret and Munné-Bosch 2015). Together with tocotrienols, tocopherols constitute the vitamin E (VTE) group of compounds, which are distinguished by the degree of saturation of their prenyl moiety and the methylation pattern of their polar head. These compounds are synthesized de novo from a hydrophilic chromanol group and a prenyl side chain produced by the shikimate and methylerythritol phosphate (MEP) pathways, respectively (Miret and Munné-Bosch 2015). For tocopherols, phytyl diphosphate (PDP) side chain prenylation by homogentisate phytyltransferase (VTE2) converts homogentisate (HGA) into 2-methyl-6-phytyl-1,4-benzoquinone (MPBQ). Tocopherol cyclase (VTE1) catalyzes chromanol ring synthesis leading to the formation of  $\delta$ -tocopherol. Alternatively, MPBQ methylation, by MPBQ methyltransferase (VTE3), results in 2,3-dimethyl-6-phytyl-1,4-benzoquinone (DMPBQ), whose cyclization

by VTE1 leads to the formation of  $\gamma$ -tocopherol. The addition of a methyl group to the sixth position of the chromanol ring, by  $\gamma$ -tocopherol methyltransferase (VTE4), converts  $\delta$ -tocopherol and  $\gamma$ -tocopherol into  $\beta$ -tocopherol and  $\alpha$ -tocopherol, respectively. In addition to the pathway of de novo synthesis, the PDP precursor may also originate from the recycling of the phytol moiety released from Chl turnover or degradation, by the action of phytol kinase (VTE5) (Valentin 2006) and phytyl phosphate kinase (VTE6) (vom Dorp et al. 2015). Tocotrienols are synthesized from the condensation of HGA with geranylgeranyl diphosphate (GGDP) by the action of a specific transferase (HGGT, homogentisate geranylgeranyltransferase). The resultant 2-methyl-6-geranylgeranyl benzoquinol (MGGBQ) is modified, in a similar manner to tocopherols, by VTE1, VTE3 and VTE4 to produce  $\alpha$ -,  $\beta$ -,  $\delta$ - and  $\gamma$ -tocotrienols.

Although most of the enzyme activities involved in the biosynthesis of tocopherols have been localized at the inner membrane of the chloroplast envelope (Spicher and Kessler 2015), the key step of cyclization is carried out by VTE1 in plastoglobules (PGs) (Vidi et al. 2006). Moreover, HGA biosynthesis occurs in the cytosol (Wang et al. 2016). These facts implicate that biosynthetic intermediates must traffic between the inner membrane and the PGs (Spicher and Kessler 2015) and between the cytoplasm and plastids (Pellaud and Mène Saffrané 2017).

The study of tocopherol-deficient plants has provided evidence concerning the exchange of chemically diverse metabolites between the plastid and extraplastidic environments. *Arabidopsis thaliana* *vte2* mutants showed altered composition of lipids, mostly of those generated via the endoplasmic reticulum (ER) pathway (Maeda et al. 2008). Similar changes in ER fatty acid profile were observed in tomato VTE5-deficient plants grown under both normal (Almeida et al. 2016), and high light and temperature conditions (Spicher et al. 2017). Genetic evidence suggests that these alterations in extra-plastidic lipid metabolism in VTE-deficient plants are mediated by ER fatty acid desaturases (Maeda et al. 2008, Song et al. 2010). This means that plastid-synthesized tocopherol, and/or its related metabolites, should be accessible for the ER, directly or indirectly influencing ER-resident enzymes. Two different, yet non-mutually exclusive models have been proposed to explain transorganellar communication: an intermembrane transporter-based model and a model based on membrane hemi-fusion between organellar membranes (Mehrshahi et al. 2014). These models could also be applicable to the intraorganellar traffic of tocopherol biosynthetic intermediates between the inner membrane and PGs described above. Although the membrane hemi-fusion model is supported by transorganellar complementation of *vte1* *Arabidopsis* mutant plants (Mehrshahi et al. 2013), neither proteins with tocopherol-related compound binding activity nor contact between the PG and envelope have been described in plants (Austin 2006). This constitutes a current research gap on intraplastidial and chloroplast–ER communication.

Previous studies using a *Solanum pennellii* introgression line population identified a major quantitative trait locus (QTL) for tomato fruit tocopherol content on chromosome 9 (Schauer et al. 2006, Almeida et al. 2011). This QTL co-localized with a

locus encoding a SEC14-like protein (Almeida et al. 2011). Some members of this protein family have been shown to be involved in tocopherol transport in mammalian cells and in lipid traffic in yeasts and plants (Saito et al. 2007, Bankaitis et al. 2010). In this work, we show that this protein, hereafter named SITBP (*Solanum lycopersicum* tocopherol-binding protein), is a homolog of the human  $\alpha$ -tocopherol transfer protein (HsTTP) (Meier et al. 2003), which has intermembrane  $\alpha$ -tocopherol transfer activity mediated by phosphatidylinositol phosphates (PIPs) (Kono et al. 2013). By functional characterization of SITBP, we provide insights about this plastidial protein involved in intracellular traffic of  $\alpha$ -tocopherol in plants.

## Results

### *SITBP* encodes a chloroplast-targeted protein of the patellin family and is highly expressed in green tissues

In order to evaluate the diversity of SEC14-like proteins in plants, the Phytozome v10.2 database was surveyed using SITBP as bait (Solyc09g015080). This sequence was found to belong to the cluster id 55282292, a gene family that comprises 286 members annotated as 'Hypothetical Viridiplantae genes' associated with lipid transport and metabolism. Of these genes, 147 sequences encompassing 24 Angiosperm species were selected on which to perform a phylogenetic analysis. Additionally, the functionally characterized SEC14 protein from *Saccharomyces cerevisiae* (Tanksley 2004), ScSEC14, and the *Homo sapiens* proteins TOCOPHEROL TRANSFER PROTEIN, HsTTP (Nava et al. 2006), and SUPERNATANT PROTEIN FACTOR, HsSPF (Stocker and Baumann 2003), were included in the analysis and used as queries for retrieving *Mus musculus*, *Drosophila melanogaster*, *H. sapiens* and *Bombyx mori* homologs (Supplementary Table S1).

The phylogenetic reconstruction revealed three clearly defined plant clades, which were named according to their *Arabidopsis thaliana* homologs (Peterman 2004, Peterman et al. 2006). ScSEC14 remained as an outgroup, while the Animalia sequences were divided into two clades, HsTTP-like and HsSPF-like, indicating an ancestral duplication within this kingdom. The clades containing AtPATL4-like and AtPATL6, with the latter including SITBP, split before the divergence of Eudicots and Monocots. Yet a duplication following the divergence of the basal order Ranunculales, which includes *Aquilegia coerulea*, increased diversity in Eudicot species originating two distinct clades, AtPATL1/2 and AtPATL3/5 (Fig. 1a).

The proteins from the plant and the Hs-SPF-like clades exhibit three known and conserved domains in all sequences: (i) a CRAL–TRIO domain (IPR001251, CELLULAR RETINALDEHYDE BINDING PROTEIN and the TRIO guanine exchange factor), which binds small lipophilic molecules such as retinaldehyde and  $\alpha$ -tocopherol (Panagabko et al. 2003); (ii) the CRAL–TRIO N-terminal domain (IPR011074), an  $\alpha$ -helix-rich region with unknown function found at the N-terminal region of CRAL–TRIO domains; and (iii) the GOLD domain (IPR009038, GOLGI DYNAMICS) that is predicted to mediate interaction with other proteins (Anantharaman and Aravind 2002) (Fig. 1a).

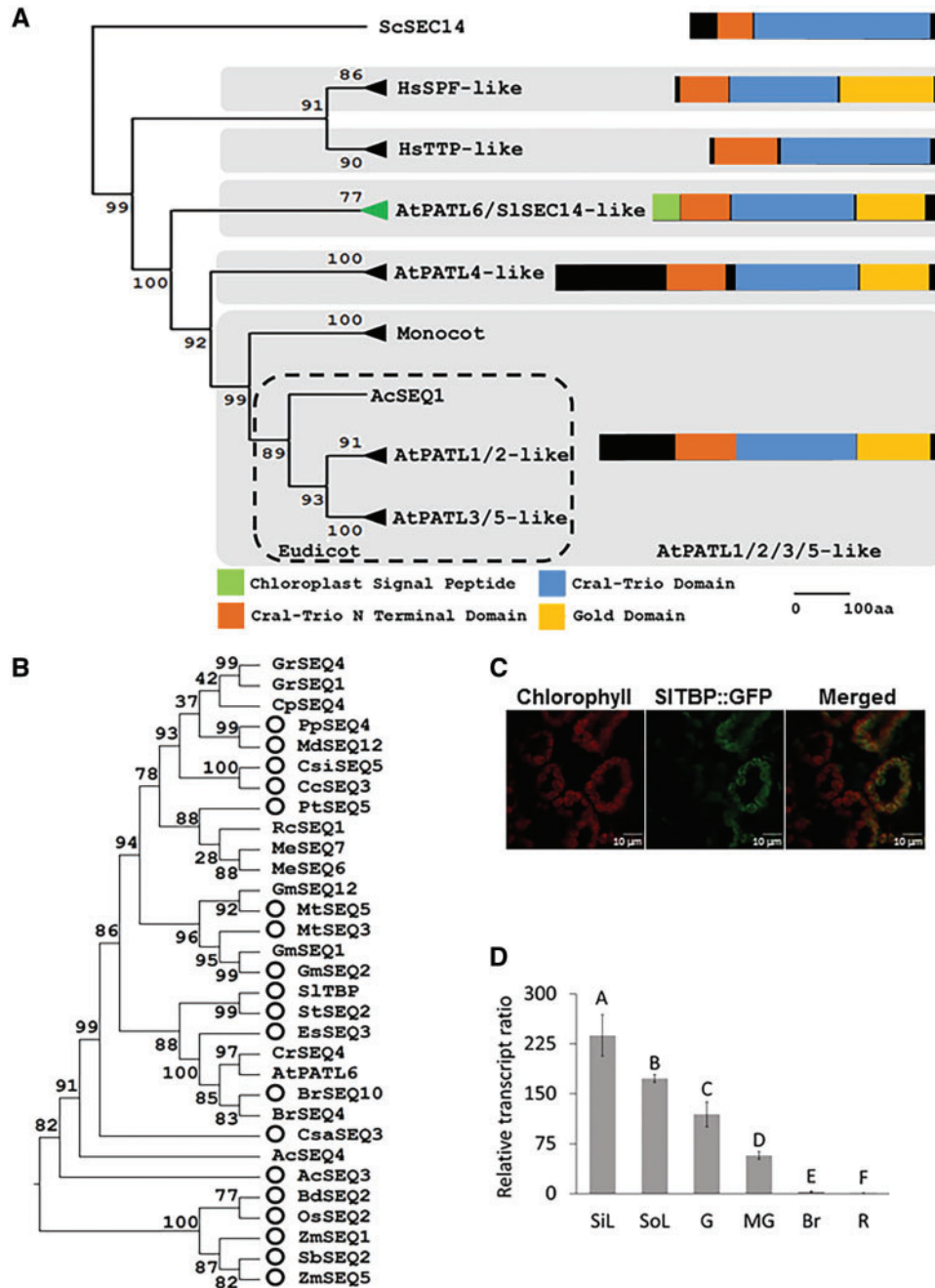


**Fig. 1** Characterization of SEC14-like proteins. (A) Phylogenetic reconstruction of SEC14-like proteins. Sequences were identified in Phytozome and the NCBI database (Supplementary Table S1). Representative protein structures for each clade are outlined on the right showing the domains: CRAL–TRIO N-terminal domain (IPR011074), CRAL–TRIO domain (IPR001251) and GOLD domain (IPR009038). Chloroplast signal peptide was identified by ChloroP software prediction (Emanuelsson et al. 1999). The SITBP-containing clade is highlighted in green. (B) Detail of the AtPATL6/SITBP-like clade. Sequences highlighted with circles are predicted to be targeted to plastids. (C) Transient expression of SITBP::GFP fusion protein in mesophyll cells of *Nicotiana benthamiana* leaves indicates chloroplast targeting under confocal microscopy examination. Chl autofluorescence, GFP fluorescence and merged signals are indicated above the panels. (D) The *SITBP* gene transcript profile in leaves and fruits. Data indicates relative expression normalized against the ripe stage. Data represent the mean  $\pm$  SE from at least three biological replicates. Letters indicate statistically different values ( $P < 0.05$ ). SiL, sink leaf; SoL, source leaf; G, green fruit stage; MG, mature green fruit stage; Br, breaker fruit stage; R, ripe fruit stage.

In order to obtain information concerning the subcellular localization of SEC14 proteins, the presence of putative plastidial signal peptides was *in silico* investigated. Of the 147 plant sequences, 22 were predicted to be plastid targeted (Supplementary Table S1). Interestingly, 19 of them are

members of the AtPATL6 SITBP clade (Fig. 1b), suggesting that this group is characterized by the presence of a chloroplast signal peptide. The prediction of SITBP as a plastidial protein was confirmed by the transient expression of a GFP (green fluorescence protein) fusion protein in *Nicotiana benthamiana*

leaves, where the confocal visualization of the fluorescence revealed that SITBP is targeted to the chloroplasts (Fig. 1c). Regarding the expression of *SITBP*, the mRNA corresponding to this gene was detected in both leaves and fruits; however, its expression levels were considerably higher in green tissues, being 250-fold more highly expressed in sink leaves than in ripe fruits (Fig. 1d).

### SITBP binds to $\alpha$ -tocopherol

Given that the *SITBP* gene was identified to be associated with a tocopherol QTL (Schauer et al. 2005, Almeida et al. 2011) and due to its homology to HsTTP (Min et al. 2003), we next explored its  $\alpha$ -tocopherol binding activity. First, we compared the predicted amino acid sequence and the 3-D structure of tomato and human polypeptides. Despite exhibiting a modest overall identity of 24.8%, structural alignment revealed that both proteins are highly similar—including the  $\alpha$ -tocopherol-binding pocket (Min et al. 2003) (Supplementary Fig. S1). Interestingly, out of the 13 residues that interact with the ligand, two are identical and seven are similar (Supplementary Fig. S1b), supporting the hypothesis of conserved function.

Based on this observation, the His-tagged tomato protein was expressed in *Escherichia coli* (BL21AI) and the production of a recombinant protein was confirmed by Western blot analysis with anti-His antibody (Fig. 2a). SITBP- $\alpha$ -tocopherol binding was tested by affinity chromatography using an  $\alpha$ -tocopherol-biotin conjugate immobilized on a streptavidin column. After loading, the column showed retention of SITBP protein until eluted with  $\alpha$ -tocopherol, as shown in Fig. 2b, confirming its ability to bind  $\alpha$ -tocopherol. It is worth mentioning that column loading and elution were performed with PBS (phosphate-buffered saline) buffer, which has no protein denaturing effect. The identity of the SITBP eluted protein (46 kDa band) was verified by mass spectrometry sequencing (Supplementary Fig. S2).

To improve the chromatography and evaluate the binding specificity, SITBP was purified and binding assays were repeated with tocopherol and another isoprenoid-derived lipophilic compound, phylloquinone. Their results showed that SITBP binding activity is not limited to tocopherol, raising the possibility that this protein might be involved in broader lipid trafficking regulation (Fig. 2c).

### SITBP-knockdown plants are deficient in tocopherol and carotenoid accumulation

Having demonstrated that SITBP binds tocopherol, the role of this protein in tomato metabolism was evaluated by the characterization of *SITBP*-knockdown plants. Four independent RNA interference (RNAi) lines, exhibiting a reduced expression of >50% in both leaves and ripe fruits, were selected for further phenotyping, hereafter referred to as L15, L18, L19 and L24 (Supplementary Fig. S3). Primary metabolism was slightly affected by the silencing of *SITBP* (Fig. 3; Supplementary Table S2). Most of the changes were observed in source leaves; 18 metabolites showed a distinct pattern of accumulation in the

leaves, while only seven were affected in ripe fruits. The metabolic classes more affected by *SITBP* knockdown were the organic acids in leaves, specifically tricarboxylic acid cycle intermediates and those involved in ascorbate metabolism. Additionally, *SITBP* deficiency led to an increase in several amino acids in both analyzed organs.

The total tocopherol content was significantly diminished in leaves and ripe fruits of the *SITBP*-knockdown lines, by approximately 30% and 20%, respectively. In contrast, Chls were unaffected by *SITBP* silencing; however, the major carotenoids, lycopene and  $\beta$ -carotene, also exhibited reduced contents in ripe fruits (Table 1).

### SITBP plays a role in maintaining chloroplast structural integrity and affects lipid composition

Given that the role of tocopherol in plant growth and development is related to the stabilization of photosynthetic membranes, gas exchange and Chl fluorescence parameters were measured in source leaves from 8-week-old *SITBP*-knockdown plants (Table 2). No differences were found in the transpiration rate ( $E$ ), stomatal conductance ( $g_s$ ) or  $CO_2$  assimilation rate ( $A$ ). However, *SITBP* deficiency resulted in reductions in the electron transport rate (ETR), the proportion of open PSII centers ( $qP$ ) and the PSII operating efficiency ( $\Phi_{PSII}$ ), while non-photochemical quenching (NPQ) and reduced quinone acceptor ( $1 - pQ$ ) were increased in comparison with the wild-type genotype. Although there were no penalties on either biomass accumulation or fruit number or weight (Supplementary Table S3), the above-mentioned results implied that *SITBP* deficiency alters the energy usage of excited Chl. Thus, as a parameter of oxidative stress, lipid peroxidation was estimated. The malondialdehyde (MDA) equivalent was more than doubled in the leaves of transgenic plants compared with the control genotype (Fig. 4a). However, no changes in lipid peroxidation were detected in fruits (Supplementary Fig. S4). Regarding the plastidial ultrastructure, *SITBP* knockdown led to a dramatic thylakoid grana disruption of the leaf chloroplasts (Fig. 4b) and the development of smaller plastids with more and larger PGs (Fig. 4c).

Having demonstrated that *SITBP* silencing affected the tocopherol levels and, consequently, impacted on photosynthetic function, lipid peroxidation and plastidial membrane ultrastructure, we next evaluated how tocopherol deficiency affects lipid metabolism. For this purpose, the lipid profile of *SITBP*-knockdown lines was analyzed (Supplementary Table S4). In source leaves, increased levels of total neutral lipids (NLs) were observed (Fig. 4d), as a consequence of the increases in fatty acid phytol esters (FAPEs), triacylglycerols (TAGs), free fatty acids (FFAs) and diacylglycerols (DAGs) (Supplementary Table S4). It is interesting to note that all the identified acyl chains (i.e. C16:0, C18:0, C18:1, C18:2 and C18:3) of the NLs increased in the transgenic lines. Regarding the fatty acid saturation level, higher linoleic acid (C18:2) total content (4.3 vs. 6.1  $\mu\text{g mg DW}^{-1}$  comparing the mean of control and transgenic lines, respectively) and a decreased C18:3/C18:2 ratio (2.0 vs. 1.5 comparing the mean of control and transgenic lines, respectively) were observed in the

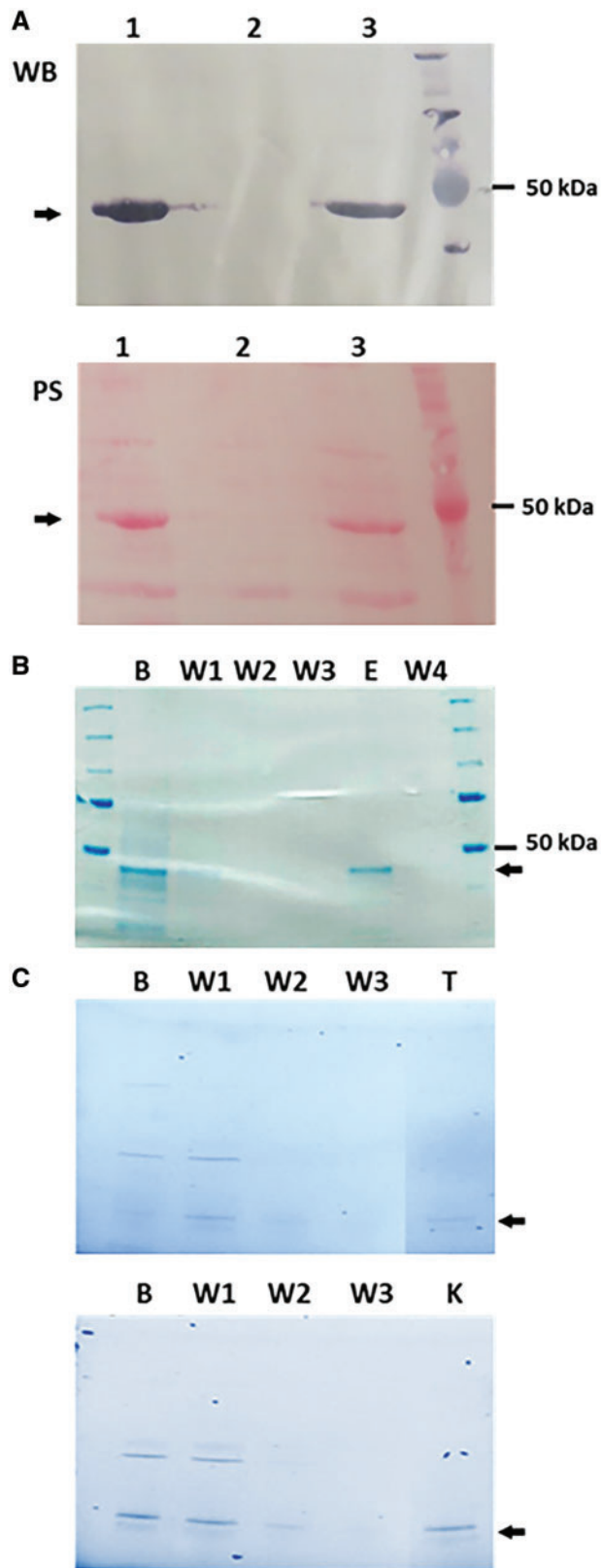


**Fig. 2** Heterologous expression of SITBP protein and binding assays. (A) Western blot (WB) and Ponceau staining (PS) of SITBP-His protein expressed in *Escherichia coli* (BL21AI strain). Western blot was performed using an anti-His antibody. Lanes 1 and 3: total protein extract from two independent *E. coli* clones expressing SITBP; Lane 2: negative control; total protein extract from an untransformed *E. coli* clone. The

leaves from *SITBP*-knockdown lines. Except for the reduction in monogalactosyldiacylglycerols (MGDGs) (composed mainly of C18:2 and C18:3), lipid profiles from ripe fruits were almost indistinguishable between transgenic and control plants; not even alterations in fatty acid saturation levels were detected (Fig. 4d).

### Expression profiles of *SITBP*-knockdown plants are in accordance with their phenotypic alterations

The effect of *SITBP* deficiency was also assessed at the level of global gene expression. In source leaves and ripe fruits, 11,474 and 11,630 genes displayed detectable expression, respectively. *SITBP* deficiency resulted in up-regulation of 261 and 419 genes and down-regulation of 139 and 429 genes, respectively, in these organs (Supplementary Table S5; Supplementary Fig. S5), only 3% and 7% of the total transcripts analyzed. Subsequently, the altered expression of approximately 70% (50/72) of tested genes was validated by means of quantitative PCR assay (Supplementary Tables S5, S6).

The classification of the genes exhibiting altered patterns of expression revealed that miscellaneous, RNA and protein metabolism as well as signaling were the functional categories most affected by *SITBP* deficiency (Supplementary Fig. S6). However, considering the metabolic perturbation induced by *SITBP* knockdown, the genes associated with photosynthesis (functional category 1 PS), tetrapyrrole metabolism (functional category 19.99 tetrapyrrole synthesis), lipid metabolism (functional category 11 lipid metabolism), isoprenoid metabolism (functional category 16.1 secondary metabolism.isoprenoids), inositol/phosphoinositide metabolism (functional categories 30.4 signaling.phosphoinositides, 3.4 minor CHO metabolism.myo-inositol and 34.2 transporter.sugars-inositol) and redox homeostasis (functional category 21 redox) categories were manually curated and the subcellular localization of their products predicted. Fig. 5 summarizes these results and shows all genes presenting altered expression in leaves (Fig. 5a) and ripe fruits (Fig. 5b) from the transgenic lines numbered according to Supplementary Table S5.

In source leaves, genes belonging to the photosynthesis-related categories (1 PS, 19 tetrapyrrole synthesis and 16.1 secondary metabolism.isoprenoids) were mostly up-regulated in the transgenic lines. These leaves also showed alterations in the expression of redox balance-related genes, such as a *GLUTAREDOXIN* (15), *PEROXIDASES* (14) and a *PHOSPHOGLUCONOLACTONASE* (13). Lipid metabolism-related genes showing altered expression in the leaves of the transgenic belong to both prokaryotic (plastidial) and

### Fig. 2 Continued

arrow indicates SITBP protein. (B) Coomassie blue-stained gel from affinity chromatography assay showing SITBP binding to  $\alpha$ -tocopherol from *E. coli* extract. B, breakthrough; W, washing steps as detailed in the Materials and Methods; E, elution with  $\alpha$ -tocopherol. The arrow indicates SITBP protein as confirmed by MALDI mass spectrometry (Supplementary Fig. S2). (C) Coomassie blue-stained gel from affinity chromatography assays showing purified SITBP binding to  $\alpha$ -tocopherol (above) and phylloquinone (below). B, breakthrough; W, washing steps as detailed in the Materials and Methods; T, elution with  $\alpha$ -tocopherol; K, elution with phylloquinone. The arrow indicates SITBP protein.

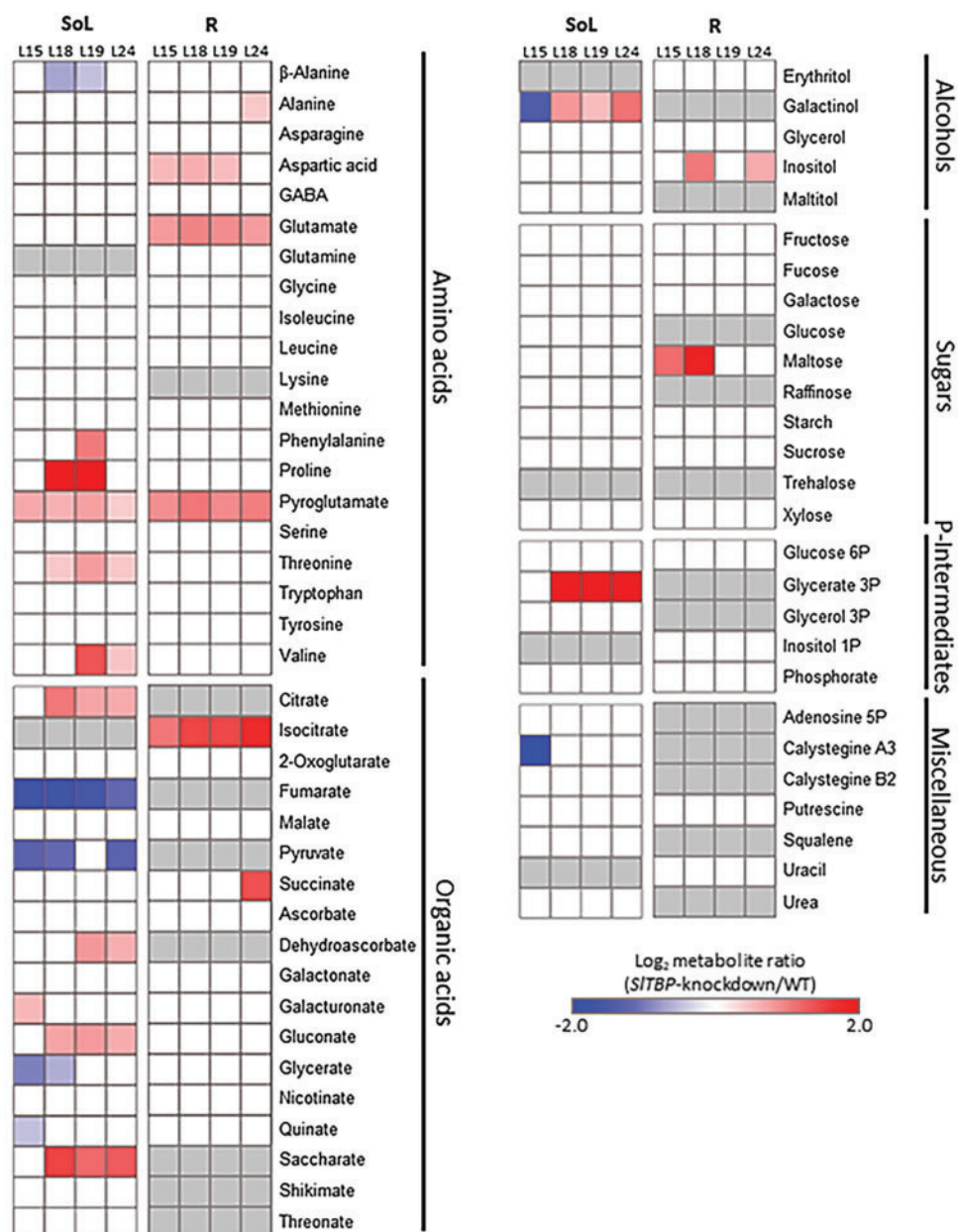


**Fig. 3** Primary metabolic profile of *SITBP*-knockdown lines. SoL, source leaves; R, ripe fruits. Data were normalized to fresh weight and are presented as the  $\text{Log}_2$  ratio between *SITBP*-knockdown plants and the wild type. All the ratio values are shown in Supplementary Table S2. Only statistically significant values compared with the wild type genotype are shown in the color gradient ( $P < 0.05$ ). Gray color indicates not detected.

eukaryotic (ER) lipid pathways and encode a wide range of biochemical functions (6, 9, 5, 8 and 7). Finally, considering that the HsTTP transports tocopherol in a PIP-mediated manner (Kono et al. 2013), the expression of the inositol/phosphoinositide-related genes was carefully inspected, and showed an altered pattern of expression for five distinct loci.

A high number of genes from the selected categories showed altered expression profiles in ripe fruits from the transgenic lines. Regarding the isoprenoids category, three genes directly involved in the carotenoid biosynthetic pathway (61, 64 and 65) and two carotenoid catabolism-associated paralogs (66) showed altered levels of their mRNA. Moreover, four other genes (62, 63, 67 and 68) involved in metabolism of terpenoids

(other than carotenoids) showed changes in their mRNA levels in the transgenics. Intriguingly, several genes associated with 13 different protein functions belonging to photosynthesis category (1 PS) exhibited altered expression. Additionally, a diverse set of genes (53, 56, 57, 58, 14, 52, 54 and 55) involved in redox regulation-associated functions showed changes in their transcript profile, being found in different cellular compartments, such as chloroplasts, plasma membrane, ER and cytosol. The functional category exhibiting the highest number of altered genes in ripe fruits from *SITBP*-knockdown plants was lipid metabolism, including genes involved in biosynthesis (e.g. acyl carriers, 41 and 42; and acyl transferases, 35) and catabolism (e.g. *LIPASE*, 6; and *LIPOXYGENASE*, 39), which were mostly

**Table 1** Pigment and tocopherol contents in *SITBP*-knockdown lines

	WT	L15	L18	L19	L24
<b>Source leaves</b>					
Chl <i>a</i> <sup>a</sup>	111.59 ± 4.86	116.55 ± 10.81	114.95 ± 7.58	115.26 ± 9.39	99.09 ± 6.01
Chl <i>b</i> <sup>a</sup>	31.30 ± 1.97	34.97 ± 3.58	33.37 ± 2.10	34.06 ± 2.73	27.08 ± 1.97
Total carotenoids <sup>a</sup>	31.69 ± 1.32	35.22 ± 2.95	33.76 ± 2.11	26.95 ± 4.18	29.71 ± 1.85
$\alpha$ -Tocopherol <sup>b</sup>	50.57 ± 2.03	<b>28.18 ± 9.08</b>	<b>41.02 ± 8.54</b>	<b>47.2 ± 0.48</b>	<b>38.67 ± 5.37</b>
$\gamma$ -Tocopherol <sup>b</sup>	3.35 ± 1.58	<b>1.00 ± 0.26</b>	2.75 ± 0.91	<b>1.44 ± 0.12</b>	<b>1.32 ± 0.40</b>
Total tocopherol <sup>b</sup>	55.64 ± 4.67	<b>29.85 ± 10.24</b>	<b>44.44 ± 9.74</b>	<b>48.67 ± 0.42</b>	<b>40.11 ± 5.30</b>
<b>Ripe fruits</b>					
$\beta$ -Carotene <sup>c</sup>	0.30 ± 0.06	<b>0.12 ± 0.01</b>	<b>0.08 ± 0.01</b>	<b>0.07 ± 0.01</b>	<b>0.07 ± 0.02</b>
Lycopene <sup>c</sup>	20.82 ± 3.57	11.28 ± 1.39	<b>8.54 ± 0.47</b>	<b>6.84 ± 1.84</b>	<b>8.89 ± 0.18</b>
$\alpha$ -Tocopherol <sup>b</sup>	17.72 ± 3.75	18.1 ± 0.33	14.66 ± 5.09	13.69 ± 2.05	<b>11.89 ± 1.82</b>
$\beta$ -Tocopherol <sup>b</sup>	0.21 ± 0.01	<b>0.27 ± 0.02</b>	0.22 ± 0.02	0.19 ± 0.04	0.20 ± 0.01
$\gamma$ -Tocopherol <sup>b</sup>	4.35 ± 0.75	4.14 ± 1.47	<b>2.94 ± 0.73</b>	<b>2.31 ± 0.10</b>	<b>3.05 ± 0.17</b>
$\delta$ -Tocopherol <sup>b</sup>	0.13 ± 0.02	0.29 ± 0.13	<b>0.09 ± 0.01</b>	0.08 ± 0.06	0.16 ± 0.03
Total tocopherol <sup>b</sup>	22.05 ± 4.49	23.52 ± 2.48	17.45 ± 6.22	<b>16.28 ± 2.05</b>	<b>15.3 ± 1.95</b>

Values are represented as means ± SD of at least three biological replicates. Values in bold denote significant differences between the wild-type (WT) and *SITBP*-knockdown genotypes ( $P < 0.05$ ).

<sup>a</sup> $\mu\text{g cm}^{-2}$ .

<sup>b</sup> $\mu\text{g g}^{-1}$  FW.

<sup>c</sup> $\text{mg } 100 \text{ g}^{-1}$  FW.

**Table 2** Gas exchange and Chl fluorescence parameters in *SITBP*-knockdown lines

	WT	L15	L18	L19	L24
qP	0.58 ± 0.01	<b>0.52 ± 0.02</b>	<b>0.50 ± 0.02</b>	<b>0.52 ± 0.03</b>	<b>0.53 ± 0.03</b>
NPQ	1.42 ± 0.09	<b>1.64 ± 0.11</b>	<b>1.57 ± 0.10</b>	<b>1.58 ± 0.12</b>	<b>1.56 ± 0.10</b>
ETR	148.70 ± 6.42	<b>131.10 ± 9.23</b>	<b>126.50 ± 7.17</b>	144.10 ± 6.14	<b>133.70 ± 8.15</b>
1 - pQ	0.43 ± 0.01	<b>0.49 ± 0.03</b>	<b>0.50 ± 0.02</b>	0.44 ± 0.02	<b>0.47 ± 0.03</b>
$\Phi_{\text{PSII}}$	0.29 ± 0.01	<b>0.25 ± 0.02</b>	<b>0.23 ± 0.02</b>	<b>0.25 ± 0.02</b>	<b>0.24 ± 0.02</b>
A	10.42 ± 1.79	7.94 ± 2.32	9.19 ± 1.89	10.51 ± 1.89	8.55 ± 1.89
$g_s$	0.07 ± 0.02	0.06 ± 0.01	0.09 ± 0.02	<b>0.14 ± 0.02</b>	0.08 ± 0.03
E	1.63 ± 0.45	1.80 ± 0.21	2.19 ± 0.3	<b>3.09 ± 0.31</b>	1.77 ± 0.47

qP =  $[(F_m' - F_s)/(F_m' - F_0')]$ , photochemical quenching; NPQ =  $[(F_m - F_m')/F_m']$ , non-photochemical quenching; ETR =  $[(F_m' - F_s)/F_m'] \times f \times l \times \alpha$ -leaf, electron transport rate; 1 - pQ =  $[(F^s - F_0')/(F_m' - F_0')]$ , reduced plastoquinones;  $\Phi_{\text{PSII}}$  =  $[(F_m' - F_s)/F_m']$ , PSII operating efficiency; A ( $\mu\text{mol CO}_2 \text{ m}^{-2} \text{ s}^{-1}$ ), CO<sub>2</sub> assimilation rate;  $g_s$  ( $\text{mmol H}_2\text{O m}^{-2} \text{ s}^{-1}$ ), leaf stomatal conductance; E ( $\text{mmol H}_2\text{O m}^{-2} \text{ s}^{-1}$ ), transpiration rate.

Data correspond to measurements in the third fully expanded leaf of 8-week-old plants and represent the means ± SD of six biological replicates. Values in bold denote significant differences between the wild-type (WT) and *SITBP*-knockdown genotypes ( $P < 0.05$ ).

up-regulated. These genes also belong to both prokaryotic (plastidial) and eukaryotic (ER) lipid pathways. Similarly, as described for leaves, inositol/phosphoinositide-related genes were also altered in the fruits of the transgenic lines.

## Discussion

In 2011, Almeida et al. identified three candidate genes within a major QTL mapped on chromosome 9 for total tocopherol content in tomato fruits. These genes were functionally characterized and demonstrated to affect this trait through different regulatory mechanisms: *SIVTE3* participates in de novo  $\alpha$ -tocopherol biosynthesis (Quadrona et al. 2014); *SIVTE5* regulates the availability of prenol precursor by Chl-derived phytol

recycling (Almeida et al. 2016); and, in this work, we present evidence concerning the functionality of *SITBP*, which encodes a protein with a novel function in plants that affects the accumulation of VTE through its  $\alpha$ -tocopherol binding activity.

Phylogenetic analysis presented here supports that *SITBP* is a member of the SEC14 protein family, which is distributed from yeast to humans and participates in PIP-mediated lipid transport (Bankaitis et al. 2010). *SITBP* belongs to the plant PATELLIN gene family, whose members have been poorly characterized to date. *Arabidopsis thaliana* PATELLIN 1 and 2 (AtPATL1/2) bind phosphoinositides and participate in vesicle trafficking events (Peterman et al. 2004) and membrane regeneration (Suzuki et al. 2016), respectively. Given that most of the proteins of the *SITBP*-containing clade are characterized by the presence of predicted chloroplast target peptides, it is more

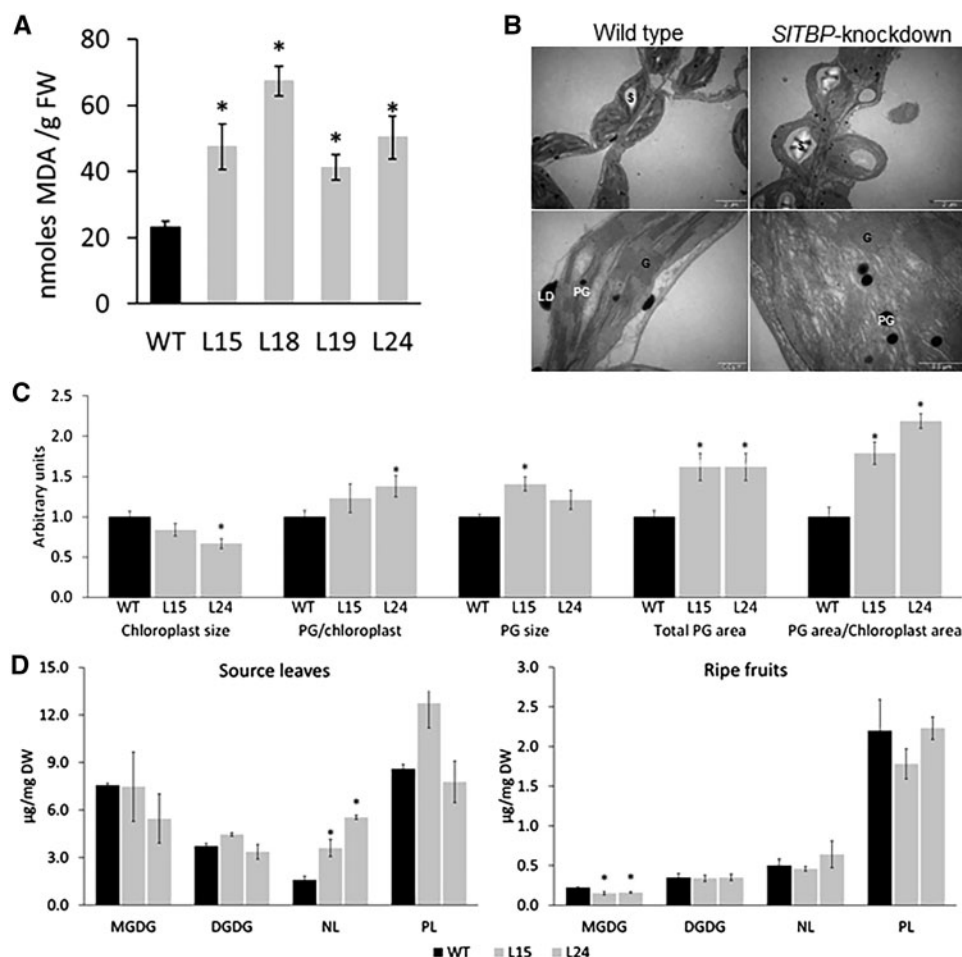


**Fig. 4** Lipid peroxidation, chloroplast structure and lipid profile of *SITBP*-knockdown lines. (A) Lipid peroxidation assay in leaves. Values represent the means  $\pm$  SE of at least three biological replicates. Asterisks denote statistically significant values compared with the wild-type (WT) genotype ( $P < 0.05$ ). (B) Chloroplast structure of wild-type and *SITBP*-knockdown leaves. G, grana; S, starch granule; LD, lipid droplet; PG, plastoglobule. (C) Chloroplast and plastoglobule (PG) size, ratio and area. Values represent the means  $\pm$  SE of at least three biological replicates. Asterisks denote statistically significant values compared with the wild-type (WT) genotype ( $P < 0.05$ ). (D) Content of the main lipid classes. MGDG, monogalactosyldiacylglycerols; DGDG, digalactosyldiacylglycerols; NL, total neutral lipids (fatty acid phytol esters, triacylglycerides, free fatty acids and diacylglycerols); PL, total phospholipids (phosphatidylglycerols, phosphatidylethanolamines, phosphatidic acids, phosphatidylinositols, phosphatidylcholines). Values represent the means  $\pm$  SE of at least three biological replicates. Asterisks denote statistically significant values compared with the wild-type (WT) genotype ( $P < 0.05$ ).

parsimonious to assume that this is an ancestral feature that was independently lost during evolution in a few members of this clade, such as the case of the *A. thaliana* ortholog (AtPATL6). Importantly, the chloroplast subcellular localization of the tomato protein was experimentally confirmed here.

A close inspection of the predicted structure of *SITBP* revealed a high conservation with the CRAL–TRIO N-terminal and CRAL–TRIO domains of the human homolog HsTTP (Meier et al. 2003), even with respect to the amino acid residues which interact with  $\alpha$ -tocopherol (Min et al. 2003). This observation led us to investigate whether *SITBP* has tocopherol binding activity, which was confirmed by means of affinity chromatography assay with the tomato recombinant protein. However, the ability of phyloquinone also to elute *SITBP* from the tocopherol–biotin conjugate, exposed a broader spectrum of ligands for this protein that could be expanded to isoprenoid-derived lipophilic compounds.

Having demonstrated that *SITBP* is able to bind  $\alpha$ -tocopherol, we further investigated the involvement of this protein in tomato plant metabolism. Analyses of RNAi-mediated *SITBP*-knockdown lines revealed significant reductions in the total tocopherol contents ( $\alpha$  and  $\gamma$  forms), both in source leaves and in ripe fruits. This result demonstrates that *SITBP* participates in the regulation of tocopherol metabolism in vivo. However, the impact of tocopherol deficiency on metabolite and transcript profiles in these organs was clearly different (discussed below), revealing a metabolic organ-specific adjustment, as we have previously reported for *SIVTE5*-silenced tomato plants (Almeida et al. 2016). In general terms, the metabolic effect of *SITBP* manipulation was more pronounced in leaves than in mature fruits; however, higher numbers of genes with altered expression levels were detected in mature fruits. This is in line with the major role of transcriptional regulation over the fruit ripening process (Giovannoni et al. 2017).



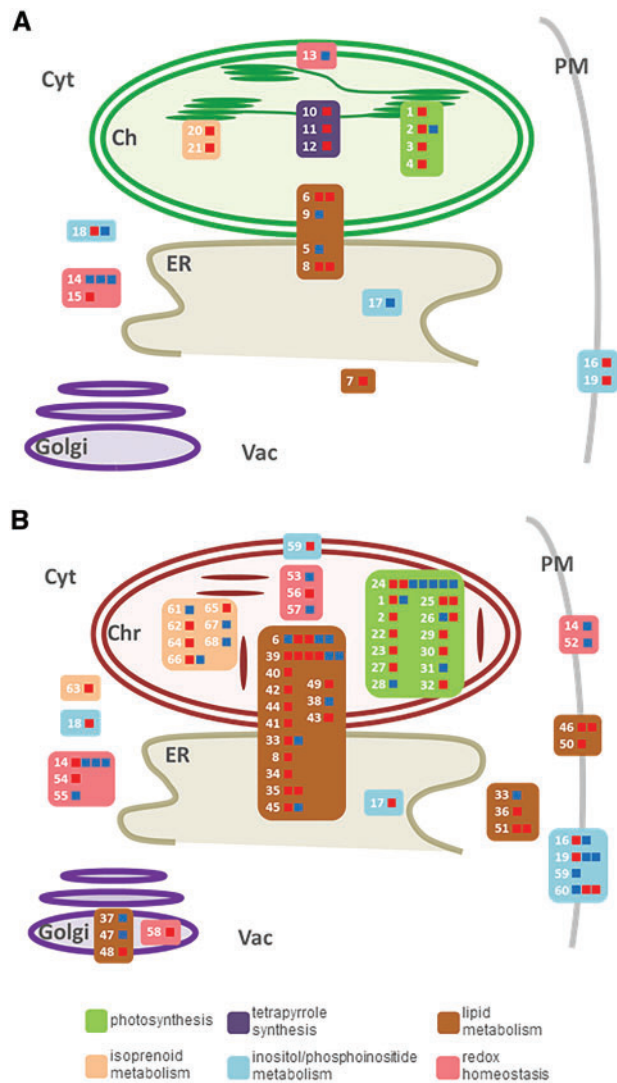


**Fig. 5** Differentially expressed genes in leaves (A) and ripe fruits (B) from *SITBP*-knockdown lines. The numbers refer to differentially expressed genes (Supplementary Table S5) within the following selected categories: photosynthesis, tetrapyrrole synthesis, lipid metabolism, isoprenoid metabolism, inositol/phosphoinositide metabolism and redox homeostasis. Ch, chloroplast; Chr, chromoplast; ER, endoplasmic reticulum; Vac, vacuole; Cyt, cytosol; PM, plasma membrane. Red and blue squares represent up- and down-regulated genes, respectively.

The role of tocopherols in protecting PSII against singlet oxygen (Krieger-Liszka and Trebst 2006) and in limiting lipid peroxidation (Miret and Munné-Bosch 2015) is well documented. Consistent with these observations, the reductions in tocopherol observed in leaves from *SITBP*-knockdown plants coincided with significant alterations in the Chl fluorescence parameters, lipid peroxidation and thylakoid membrane stacking. The changes observed in the expression of photosynthesis-related genes are in clear agreement with the observed impairments in photosynthetic light reactions, implying that the transgenic plants cannot cope with the excited Chl. This hypothesis is supported by the up-regulation of the *MENAQUINONE METHYLTRANSFERASE*-encoding gene (21 in

**Fig. 5**). This gene product participates in the biosynthesis of phyloquinone, which is a PSI-associated electron acceptor. Within this context, it is important to note that phyloquinone and tocopherols are produced into the plastoglobuli and share biosynthetic precursors (Spicher and Kessler 2015).

Beside the aforementioned phenotypes, the leaves of the transgenic plants exhibited increased levels of neutral lipids (i.e. FAPes, TAGs, FFAs and DAGs) which could explain the increase in the number and size of PGs where these compounds are stored (Nacir and Bréhélin 2013). In line with these structural and biochemical changes are the alterations in the mRNA levels of a *LIPASE* (6) and a *PHOSPHOLIPASE* (7) genes, whose products are enzymes involved in TAG and DAG NL metabolism (Padham et al. 2007, Yang et al. 2017). Furthermore, the impairment of tocopherol biosynthesis/accumulation may result in increases in free phytol—a long chain alcohol molecule—which exerts detergent-like effects which are detrimental to membrane function (Löbbecke and Cevc 1995, Sikkema et al. 1995). In contrast, FAPes, which lack detergent-like structure, also increased in the leaves of transgenic plants; however, these are not considered toxic and, in addition, they are sequestered in PGs (Lippold et al. 2012).

In accordance with the photoinhibition phenotype displayed by the transgenic plants, cellular redox homeostasis-related genes and metabolites were significantly altered. The most obvious are the cases of dehydroascorbate, *GLUTAREDOXIN* (15) and *PEROXIDASE* genes (14) (Foyer and Shigeoka 2011). An interesting example is the change in the transcript level of the *PHOSPHOGLUCONOLACTONASE* (13) gene and its corresponding product, gluconate. This enzyme of the oxidative pentose phosphate pathway is sensitive to the redox cellular homeostasis (Hölscher et al. 2014).

In ripe fruits of *SITBP*-knockdown lines, reductions in lycopene and  $\beta$ -carotene contents were observed. Two carotenoid cleavage dioxygenase- (*CCD*) encoding genes, *SICCD1* and *SICCD4* (66), were up- and down-regulated, respectively, in the fruits of these plants. Plant *CCDs* are divided into four groups, *CCD1*, *CCD4*, *CCD7* and *CCD8*, that exhibit substrate promiscuity (Auldrige et al. 2006). *CCD4* activity was reported to have a negative effect on  $\beta$ -carotene contents in *A. thaliana* seeds (Gonzalez-Jorge et al. 2013), while *SICCD1* cleaves  $\beta$ -carotene and lycopene (Simkin et al. 2004). Thus, the altered expression of *SICCD* genes might, at least partially, explain the reduced levels of carotenoids observed in ripe fruits from transgenic plants. The up-regulation of *LYCOPENE  $\beta$ -CYCLASE* (65) and *PHYTOENE SYNTHASE* (64) and the down-regulation of the *LYCOPENE  $\epsilon$ -CYCLASE* (61) gene might represent a compensatory mechanism to ameliorate the reduction observed in pigment content. Additionally, the induction of *FARNESYL DIPHOSPHATE KINASE* (63) and  *$\beta$ -OCIMENE SYNTHASE* (62) diverts the primary isopentenyl diphosphate precursor from carotenoid biosynthesis towards the production of other terpenoids, such as sitosterol and  $\beta$ -ocimene, respectively (Dudareva et al. 2003, Keim et al. 2012). This shift in carotenogenesis observed in the ripe fruits of the *SITBP*-knockdown plants is suggestive of ripening delay, which means retardation in dismantling of the photosynthetic machinery, explaining the altered expression of a high

number of photosynthesis-associated genes. It is widely known that carotenoids and tocopherols are major components of the antioxidant machinery in response to photooxidative deleterious effects. In green tissues, a boost in the xanthophyll cycle is a compensatory mechanism to palliate tocopherol deficiency (Havaux et al. 2005, 2007). However, even when ripening has been described as an oxidative phenomenon (Andrews et al. 2004), such compensatory mechanism(s) is unknown in fruits. Our transcript profiling data showed that tocopherol and carotenoid deficiency lead to a considerable alteration in the expression of redox-associated genes as a response to maintain oxidation–reduction balance.

It has been shown that tocopherol deficiency affects extra-plastidial fatty acid metabolism (Maeda et al. 2008, Almeida et al. 2016). The transcriptional profile of *SITBP*-silenced plants demonstrated that alterations in lipid metabolism occurred in those genes involved in both prokaryotic and eukaryotic pathways. Knowing that the fatty acids that support galactolipid synthesis for plastidial membranes are desaturated in the ER (Li-Beisson et al. 2010), the reduced levels of MGDG and the altered expression of the *MONOGALACTOSYLDIACYLGLYCEROL SYNTHASE*-encoding gene (43) observed in ripe fruits probably reflects that plastid–ER interorganellar communication is altered in *SITBP*-deficient plants.

Moreover, not only in fruits but also in leaves, the shift in the expression of *PHOSPHOINOSITIDE KINASE* (18) and *PHOSPHATASE* (16 and 60) encoding genes suggests that PIPs metabolism is altered in transgenic plants (Stevenson et al. 2000). Reinforcing this, higher contents of inositol were detected in ripe fruits of *SITBP*-knockdown lines. It is worth mentioning that several SEC14-like proteins have been reported to bind PIPs (Schaaf et al. 2008, Miller et al. 2015, KF de Campos and Schaaf 2017). In particular, HsTTP promotes the intermembrane release of  $\alpha$ -tocopherol in a PIP-dependent manner, and the three arginine residues (R59W, R192H and R221W) essential for PIP binding activity (Kono et al. 2013) are conserved in *SITBP*. The sequence conservation suggests that *SITBP* could have a similar reaction mechanism to that described for the human homolog.

Evidence presented here concerning the functionality of *SITBP* can be summarized as follows: (i) *SITBP* is structurally similar to HsTTP, targeted to chloroplasts and binds tocopherol; (ii) *SITBP* silencing results in a tocopherol deficiency phenotype both in leaves and fruits; (iii) the knockdown plants display alterations in chloroplast ultrastructure and Chl fluorescence parameters compatible with dysfunctional light reactions; (iv) *SITBP* deficiency results in changes in lipid metabolism in both leaves and fruits; and (v) all these changes are accompanied by variations in PIP-related gene expression. Taking all these results together, two possible scenarios for the action of *SITBP* can be proposed. First, *SITBP* could be involved in tocopherol/PIP-mediated chloroplast–ER communication and, under *SITBP* deficiency, lipid metabolism is affected, impacting on chloroplast ultrastructure, which in turn compromises tocopherol biosynthesis. The resulting reduction in antioxidant capacity impacts on the functionality of the photosynthetic light reaction machinery. The second possible model

implies that *SITBP* mediates the transport of  $\alpha$ -tocopherol (and/or its biosynthetic intermediates/or related lipophilic molecules) between the inner envelope membrane and PGs/thylakoid membranes. Thereafter, in the face of *SITBP* reduction, tocopherol accumulation is compromised, PG function is altered, leading to an impairment of the plastidial electron transport chain, and extra-plastidial lipid metabolism is affected. The disturbed plastid ultrastructure could be the consequence of the alteration in oxidative stress and/or of the shift in lipid metabolism.

The collection of evidence as a whole, rather than any single individual piece, allow us to propose that *SITBP* plays a novel function in plants, mediating the role of tocopherol in inter-/intraorganellar communication. This not only brings new insights on the intracellular traffic of non-polar compounds, but also adds another dimension on the regulation of tocopherol metabolism which should be considered for crop nutritional improvement strategies.

## Materials and Methods

### Phylogenetic analysis

The protein sequences of all members of the SEC14 gene family in plants were obtained from the Phytozome v10.2 gene family data set using the sequence of *SITBP* as query. Sequences with less than half of the length mode (i.e. 213 amino acids) were removed from the analysis. Sequences of *M. musculus*, *D. melanogaster*, *H. sapiens* and *B. mori* were obtained from a BLASTp against the NCBI (<https://www.ncbi.nlm.nih.gov>) protein database using the functionally characterized ScSEC14, HsTTP and HsSPF as queries. Only BLAST hits with a score of at least 100 were included in the analysis. Sequences were aligned by the ClustalW program in MEGA 6.0.5 software (Tamura et al. 2013), which was also used for the determination of the best substitution model for phylogenetic analysis. This reconstruction was made using the Maximum Likelihood principle with PhyML 3.0 software (Guindon et al. 2010) within the Phylogeny.fr server [<http://phylogeny.lirmm.fr/phylo.cgi/index.cgi>] (Dereeper et al. 2008); the statistical test for branch support was a parametric  $\chi^2$ -based test with the substitution model pointed out by the former analysis. The obtained tree was visualized and edited in MEGA 6.0.5 software.

For sequence annotation, domains were predicted by InterProScan 5 (Jones et al. 2014) and ScanProsite (de Castro et al. 2006) and the presence of a chloroplast signal peptide was evaluated using ChloroP (Emanuelsson et al. 1999). The protein representation was created with Prosite MyDomains - Image Creator (<http://prosite.expasy.org/mydomains/>).

### Expression of *SITBP* in *Escherichia coli*

The full-length coding region of *SITBP* was amplified with the primers indicated in Supplementary Table S9 and cloned into the pDEST17 destination vector according to the manufacturer's instructions (Gateway<sup>®</sup> Technology, Invitrogen) using LR clonase (Invitrogen). The pDEST17-*SITBP* expression clone was transferred to *E. coli* strain BL21AI by the heat shock

method as described by the supplier (Invitrogen), and the recombinant expression vectors were confirmed by PCR and digestion. Protein expression was determined as described by the supplier. Briefly, a clone was grown overnight in LB medium containing  $100 \text{ mg ml}^{-1}$  ampicillin at  $37^\circ\text{C}$  and shaken at 180 r.p.m. Subsequently, cultures were diluted 1:20 in fresh LB that contained  $100 \text{ mg ml}^{-1}$  ampicillin and cultivated at  $37^\circ\text{C}$  until the  $\text{OD}_{600}$  of the media reached 0.4. Recombinant fusion protein expression was then induced by the addition of 0.2% L-arabinose and cells were grown for 4 h. Induced cultures were centrifuged at full speed, after which the supernatant was aspirated and conserved as the soluble fraction and frozen at  $-80^\circ\text{C}$  for subsequent Western blot or binding assays. The recombinant protein was confirmed by Western blot with anti-His antibody (GE Healthcare # 27-4710-01). As the negative control, an untransformed *E. coli* (BL21AI) clone was used. For the SITBP purification, expression was performed via autoinduction in ZYM 5052 medium (1 liter of medium in a 2.5 liter flask) supplemented with  $50 \mu\text{g ml}^{-1}$  kanamycin. The medium was inoculated with 20 ml of overnight culture (BL21 DE3, pET-28a Vector), incubated 4 h at  $37^\circ\text{C}$  and 280 r.p.m., and then cooled down to  $22^\circ\text{C}$  overnight. The expression was stopped approximately 18 h after inoculation (no significant change for  $\text{OD}_{600}$  was detectable) and the cells were harvested at 6,500 r.p.m. for 30 min at  $4^\circ\text{C}$ . Pellets were collected and stored at  $-18^\circ\text{C}$  until lysis and purification.

### SITBP purification

About 40 g of the frozen pellet was resuspended in 400 ml of lysis buffer ( $2\times$  PBS, 20 mM imidazole, pH 7.5) via stirring at  $4^\circ\text{C}$  overnight. Resuspended cells were lysed by physical disruption with the following method: a scoop tip of DNase to the cell suspension was added, about 1,600 bar was applied and the suspension was allowed to flow into ambient pressure. In doing so, the rapid pressure release led to cell lysis. This was repeated twice with the cell suspension and then 2% (w/v) Triton X-100 was added. The lysed cell suspension was stirred for 1 h at  $4^\circ\text{C}$  and then centrifuged at  $9,000\times g$  for 30 min at  $4^\circ\text{C}$ . The supernatant was collected and applied on a His60 Ni Superflow resin. After the total suspension volume had passed through, the column was washed with wash buffer ( $2\times$  PBS, 40 mM imidazole, pH 7.5) until the absorption at 280 nm remained stable, which indicates that everything unspecific is washed from the column. In the last step, the protein was eluted from the Ni column with elution buffer ( $2\times$  PBS, 300 mM imidazole, pH 7.5), supplemented with 20 U of thrombin (digestion of the His-tag), and dialyzed in 4 liters of  $1\times$  PBS (pH 7.5) overnight at  $4^\circ\text{C}$  to remove the imidazole and provide optimal reaction conditions for the thrombin cleavage.

### Synthesis of biotinylated tocopherol

To synthesize (*R*)-2,5,7,8-tetramethyl-2-[(4*R*,8*R*)-4,8,12-trimethyltridecyl]chroman-6-yl 5-[(3*aS*, 4*S*, 6*aR*)-2-oxohexahydro-1*H*-thieno[3,4-*d*]imidazol-4-yl]pentanoate, 1.5 ml of anhydrous dimethylformamide (DMF) and 1.0 ml of anhydrous dichloromethane were added to a solution of biotin (55.8 mg,

$228 \mu\text{mol}$ ) under an inert atmosphere. Triethylamine ( $45 \mu\text{l}$ ,  $325 \mu\text{mol}$ ) was added and the solution was cooled to  $0^\circ\text{C}$  with stirring. Isobutyl chloroformate ( $45 \mu\text{l}$ ,  $344 \mu\text{mol}$ ) was added dropwise and the mixture was stirred for 45 min at  $0^\circ\text{C}$ . (+)  $\alpha$ -Tocopherol (21.4 mg,  $49.7 \mu\text{mol}$ ) and 4-(dimethylamino)-pyridine (2.0 mg,  $16.4 \mu\text{mol}$ ) were dissolved in 1.4 ml of anhydrous dichloromethane and added to the solution. The resulting mixture was stirred at  $21^\circ\text{C}$  for 2 d. The solution was partially concentrated in vacuum, then diluted with ethyl acetate (50 ml) and washed with water. The aqueous layer was then extracted with ethyl acetate ( $3\times 50 \text{ ml}$ ). The organic phase was dried over sodium sulfate, filtered and concentrated in a vacuum. The residue was purified by flash chromatography (heptane/AcOEt, 7:3 v/v) to yield the tocopherol-biotin conjugate as a colorless solid (7.7 mg,  $11.7 \mu\text{mol}$ , 24%). The resulting conjugate was confirmed by mass spectrometry (MS) and nuclear magnetic resonance (NMR) (Supplementary Fig. S7).

### Affinity chromatography

**Protein extract and  $\alpha$ -tocopherol.** A 1 ml column volume (CV) of a HiTrap<sup>TM</sup> Streptavidin HP column (GE Healthcare Bioscience AB) was flushed with  $1\times$  PBS buffer (10 CVs,  $1 \text{ ml min}^{-1}$ ). The tocopherol-biotin conjugate (31 mg,  $47.1 \mu\text{mol}$ ) was dissolved in 22 CVs of DMF/PBS buffer (1/10) and applied on the column (10 CVs,  $0.1 \text{ ml min}^{-1}$ ). Subsequently, the column was washed with PBS buffer (6 CVs), which has no protein denaturing effects. Total protein extract of the BL21AI bacteria overexpressing SITBP (0.75 ml,  $\sim 0.75 \text{ mg}$ ) was applied on the column and the flowthrough collected. The column was incubated for 10 min at  $21^\circ\text{C}$  and then washed three times with 3 CVs of  $1\times$  PBS buffer (collected as washing step 1–3). The protein was eluted with 2 CVs of  $\alpha$ -tocopherol (21 mg in 10 ml of PBS, 4.9 mM), followed by a washing step (3 CVs, collected as washing step 4). The fractions were analyzed by SDS-PAGE (7.5%, Bio-Rad pre-cast gel). A  $15 \mu\text{l}$  aliquot of each fraction was treated with 5  $\mu\text{l}$  of loading buffer ( $4\times$ ) and 1  $\mu\text{l}$  of dithiothreitol (DDT; 100 mM), heated for 5 min at  $95^\circ\text{C}$  and 10  $\mu\text{l}$  was loaded on the gel. The SDS-polyacrylamide gel was stained with Coomassie blue. The identity of the eluted protein was confirmed by MALDI mass spectrometry peptide mapping and sequencing (MALDI-MS/MS) according to Alphalyse<sup>TM</sup> (www.alphalyse.com).

**Purified SITBP and  $\alpha$ -tocopherol.** A 1 ml CV of a HiTrap<sup>TM</sup> Streptavidin HP column (GE Healthcare Bioscience AB) was flushed with  $1\times$  PBS buffer (10 CVs,  $1 \text{ ml min}^{-1}$ ). The tocopherol-biotin conjugate (31 mg,  $47.1 \mu\text{mol}$ ) was dissolved 500  $\mu\text{l}$  of DMF and applied on the column. Subsequently, the column was washed with PBS buffer (6 CVs). Purified SITBP (1 ml,  $200 \mu\text{g ml}^{-1}$ ) was applied in the column and the flowthrough collected. The column was incubated for 30 min at  $21^\circ\text{C}$  and then washed five times with 5 CVs of  $1\times$  PBS buffer (collected as washing step 1–5). The column was then eluted with 1 ml of blank (PBS with 1% Tween-20). Subsequently, the protein was eluted with 2 CVs of  $\alpha$ -tocopherol (21 mg in 10 ml of PBS with 1% Tween-20, 4.9 mM), collected as tocopherol elution, followed by a washing step (3 CVs, collected as washing step 6).

The fractions were analyzed by SDS–PAGE (7.5%, Bio-Rad stain-free pre-cast gel). A 15  $\mu$ l aliquot of each fraction was treated with 5  $\mu$ l of loading buffer (4 $\times$ ) and 1  $\mu$ l of DDT (100 mM), heated for 5 min at 80°C and 10  $\mu$ l was loaded on the gel. SDS–PAGE was visualized with the Gel Doc™ EZ System.

**Purified SITBP and phyloquinone.** A 1 ml CV of a HiTrap™ Streptavidin HP column (GE Healthcare Bioscience AB) was flushed with 1 $\times$  PBS buffer (10 CVs, 1 ml min<sup>-1</sup>). The tocopherol–biotin conjugate (31 mg, 47.1  $\mu$ mol) was dissolved in 500  $\mu$ l of DMF and applied on the column. Subsequently, the column was washed with PBS buffer (6 CVs).

Purified SITBP (1 ml, 200  $\mu$ g ml<sup>-1</sup>) was applied on the column and the flowthrough collected. The column was incubated for 30 min at 21°C and then washed five times with 5 CVs of 1 $\times$  PBS buffer (collected as washing step 1–5). The column was then eluted with 1 ml of blank (PBS with 1% Tween-20 and 1% DMF). Subsequently, the protein was eluted with 2 CVs of phyloquinone (22 mg in 10 ml of PBS with 1% Tween-20 and 1% DMF, 4.9 mM), collected as phyloquinone elutions 1 and 2, followed by a washing step (2 CVs, collected as washing step 6). Then the remaining protein was eluted with  $\alpha$ -tocopherol (21 mg in 10 ml of PBS with 1% Tween-20, 4.9 mM), collected as tocopherol elution. The fractions were analyzed by SDS–PAGE (7.5%, Bio-Rad stain-free pre-cast gel). A 15  $\mu$ l aliquot of each fraction was treated with 5  $\mu$ l of loading buffer (4 $\times$ ) and 1  $\mu$ l of DDT (100 mM), heated for 5 min at 80°C and 10  $\mu$ l was loaded on the gel. SDS–PAGE was visualized with the Gel Doc™ EZ System.

### Plant material

Tomato, *Solanum lycopersicum* L. (cv MoneyMaker), and *Nicotiana benthamiana* seeds were obtained from Meyer Beck (Berlin). *Solanum lycopersicum* (inbred variety M82, Acc LA3475) used for SITBP expression analysis was kindly provided by C.M. Rick, Tomato Genetics Resource Center (TGRC). Plants were grown under greenhouse conditions: 16/8 h photoperiod, 24  $\pm$  3°C, 60% humidity and 140  $\pm$  40  $\mu$ mol m<sup>-2</sup> s<sup>-1</sup> incident photoirradiance in 20 liter and 1 liter pots for tomato and *N. benthamiana*, respectively.

Because the T<sub>0</sub> regenerated plants produced unviable seeds (Supplementary Table S7), transgenic plants, and the corresponding controls, were phenotypically characterized in the first cutting propagation obtained from T<sub>0</sub> plants. The tocopherol deficiency phenotype was confirmed in subsequent cutting experiments (Supplementary Table S8). All assays were performed with 4–8 biological replicates per genotype. Tomato source and sink leaves were sampled from the second and third leaflets of the third totally expanded leaf and of 50% expanded leaves of 4-week-old plants, respectively. Ripe fruits were collected at 52 d after anthesis. Samples were immediately frozen in liquid N<sub>2</sub> and stored at –80°C until further processing.

Six-month-old plants were harvested, and fresh aerial biomass was measured for harvest index determination according to the following formula: harvest index = (fruit fresh mass  $\times$  100)/total aerial biomass.

### Quantitative PCR (qPCR)

RNA extraction, cDNA synthesis and qPCR assays were performed as previously described (Almeida et al. 2016). Primer sequences are listed in Supplementary Table S9. Expression values were normalized against the geometric mean of two reference genes, CAC and EXPRESSED for fruits, and ELONGATION FACTOR 1- $\alpha$  (EF1- $\alpha$ ) for leaves (Quadrona et al. 2013). A permutation test lacking sample distribution assumptions (Pfaffl et al. 2002) was applied to detect statistically significant differences ( $P < 0.05$ ) in expression ratios using the algorithms in the fgStatistics software package (<http://sites.google.com/site/fgStatistics/>).

### Cloning procedures

For SITBP subcellular localization experiments, a fragment of 1,272 bp spanning the 424 amino acids of the protein was amplified and cloned into the pK7FWG2 binary vector (Karimi et al. 2002) using the primers indicated in Supplementary Table S9, resulting in a C-terminal GFP fusion protein (pK7FWG2-SITBP) (de Godoy et al. 2013). For RNAi silencing, a 224 bp fragment of the SITBP gene was used to generate a hairpin construct. To avoid off-target effects, the construct was designed to have minimal complementarity with other genes, and then the sense/antisense fragment was used as query for a BLAST search against the Sol Genomics Network database. Six genes matched, only one with >20 nucleotides and none with at least 20 consecutive nucleotides. Thus, it is unlikely that these are off-target effects. The fragment was amplified with the primers listed in Supplementary Table S9 and cloned into pK7GWIWG2(I) binary vector (Karimi et al. 2002) to generate a hairpin construct (pK7GWIWG2(I)-SITBP) (de Godoy et al. 2013). Binary vectors were introduced into *Agrobacterium tumefaciens* strains GV3101 and GV2260 for subcellular localization and plant stable transformation, respectively.

### *N. benthamiana* transient transformation and confocal microscopy

The *Agrobacterium* strain containing pK7FWG2-SITBP was grown and infiltrated into leaves of 6-week-old *N. benthamiana* plants (de Godoy et al. 2013). After 48 h, the infiltrated tissues were observed with a Zeiss LSM 400 confocal laser microscope under a  $\times$ 63 water objective. Chl images were captured over 590 nm after excitation at 543 nm, while those for the SITBP::GFP fusion were captured over the 505–550 nm range after excitation at 488 nm with an argon laser beam.

### Plant transformation

Seedling cotyledons of *S. lycopersicum* (cv. MoneyMaker) were used as explants to generate transgenic tomato plants with the hairpin construct pK7GWIWG2(I)-SITBP by *Agrobacterium*-mediated transformation (Nunes-Nesi et al. 2005). The presence of the transgene was confirmed by PCR with the 35S promoter and specific reverse primers (Supplementary Table S9).

## Tocopherol and pigment quantification

Tocopherols were extracted and quantified by HPLC (Almeida et al. 2011). Carotenoid and Chl extraction and quantification for leaves were performed according to protocols previously described (Lichtenthaler 1987). In ripe fruits,  $\beta$ -carotene and lycopene quantification was performed by HPLC (Heredia et al. 2009).

## Photosynthetic parameters

Gas exchange and Chl fluorescence parameters were measured in the third fully expanded leaf of 8-week-old plants using a portable open gas-exchange system incorporating infra-red CO<sub>2</sub> and water vapor analyzers (LI-6400XT system; LI-COR) equipped with an integrated modulated Chl fluorometer (LI-6400 40; LI-COR) (de Godoy et al. 2013).

## Transmission electron microscopy

Source leaves from three biological replicates of *SITBP*-knock-down transgenic lines L15 and L24 were fixed, embedded in Spurr resin and ultrathin sections analyzed with a Zeiss EM 900 transmission electron microscope (Lira et al. 2017). For chloroplast and PG counting, an area determination ImageJ software was used (<http://rsb.info.nih.gov/ij/>). Pictures of 24 chloroplasts along the tissue were taken, 12 close to the cuticle and 12 from the fifth cell's layer. All PGs inside each chloroplast were counted and measured.

## Lipid peroxidation assay

Fresh vegetable material (500 mg for leaves and 1 g for fruits) was homogenized with 5 ml of cold Tris-HCl 20 mM pH 4, containing 10  $\mu$ l of 0.5 M BHT (butylated hydroxytoluene). Trichloroacetic acid (TCA) was added to 20% final concentration for protein precipitation. After centrifugation for 4 min at 12,000 $\times$ g, the thiobarbituric acid (TBA) assay was performed in the supernatants as previously described (Heath and Packer 1968). The MDA equivalent was calculated according to the Lambert and Beer formula:  $A = \epsilon \times l \times c$ , where  $A$  is the absorbance at 535 nm,  $\epsilon$  is the molar extinction coefficient ( $1.56 \times 10^5$  M cm<sup>-1</sup>),  $l$  is the path length of the cuvette (1 cm) and  $c$  is the accurate MDA concentration to be determined.

## Lipid profiles

Lipids were extracted from approximately 50 mg of lyophilized leaf or pericarp, according to (Folch 1987). Briefly, samples were incubated at 65°C during 20 min in 2 ml of isopropanol. A 2 ml aliquot of chloroform and 1 ml of H<sub>2</sub>O were then added and mixed. The organic phase was collected and washed with 1 ml of 1 M KCl. Then, the organic phase was evaporated and lipids were resolubilized with CHCl<sub>3</sub>:MeOH (2:1, v/v). Lipids were then sprayed by Linomat 5 (Camag) onto silica plates and separated by thin-layer chromatography (TLC) in parallel with lipid standards, using Vitiello-Zanetta solvent mixture (Deranieh et al. 2013) or Juguelin reagent (Juguelin et al. 1986) for polar or neutral lipids, respectively. Lipids were revealed by exposure

under UV illumination after incubation of the plates in a solution of 0.001% (w/v) primuline. The areas on the silica plates corresponding to the different lipid classes were scraped separately and incubated with 1 ml of MeOH, 2.5% H<sub>2</sub>SO<sub>4</sub> (v/v) and C17:0 at 5  $\mu$ g ml<sup>-1</sup> as internal standard in hermetically closed tubes for 1 h at 80°C. Fatty acid methyl esters (FAMES) were then extracted in 400  $\mu$ l of hexane and analyzed by gas chromatography performed using an Agilent 7,890 gas chromatograph equipped with a Carbowax column (15 m  $\times$  0.53 mm, 1.2  $\mu$ m; Alltech Associates) and flame ionization detection. The temperature gradient was 160°C for 1 min, increased to 190°C at 20°C min<sup>-1</sup>, increased to 210°C at 5°C min<sup>-1</sup> and then kept at 210°C for 5 min. FAMES were identified by comparing their retention times with commercial fatty acid standards (Sigma-Aldrich) and quantified using ChemStation (Agilent) to calculate the peak surfaces, and then comparing them with the C17:0 response.

## Microarray hybridization

Gene expression was profiled by microarray from three biological replicates of L15, L18, L24 and control plants for leaves and ripe fruit organs. Each replicate was composed of a pool of samples collected from two plants. RNA pools (1  $\mu$ g of each genotype) were amplified and aminoallyl labeled using the MessageAmp II aRNA kit (Ambion) and 5-(3-aminoallyl)-2'-dUTP following the manufacturer's instructions. A 10  $\mu$ g aliquot of aminoallyl-labeled amplified RNA was labeled with Cy5 (Reactive Dye Pack; Amersham). An equal quantity of control RNA pool was labeled with Cy3. Equal mixtures of labeled RNA were hybridized to tomato long-mer oligoarray (70 bp) slides (Microarrays Inc.) representing 12,160 genes. Hybridizations were carried out in 100  $\mu$ l of hybridization solution (5 $\times$  SSC, 0.1% SDS, 40% formamide) containing 100 pmol of Cy3- and Cy5-labeled samples, and incubated at 42°C in a thermal bath for 16 h. Then the slides were washed with 2 $\times$  SSC, 0.1% SDS four times for 10 min. Six additional washes (three with 0.1 $\times$  SSC, 0.1% SDS, and three with 0.1 $\times$  SSC, for 10 min each) at room temperature were performed before drying the glass slides with a brief centrifugation. Slides were scanned at 532 and 635 nm with a ScanArray Gx scanner at 10  $\mu$ m resolution, 90% laser power and different photomultiplier values to adjust the ratio intensity to 1.0. Raw signal intensity values were computed from the scanned array images using the image analysis software ScanArray Express (Pelkin Elmer). File data were analyzed by the Robin software package (Lohse et al. 2010) using default settings for two-color microarray analysis. Briefly, intensity raw data were collected, background-subtracted, normalized within each array by the print tip-wise normalization method (Yang et al. 2002), and subsequently scaled across all arrays to have the same median absolute deviation (Yang et al. 2002, Smyth and Speed 2003). To detect differentially expressed genes (DEGs), a linear model-based approach (Smyth 2004) was applied to compare the mean normalized values for a gene between experimental groups (transgenic and control). Mean values of DEGs were calculated from each

sample as Log<sub>2</sub> values. A gene was considered differentially expressed when its mRNA accumulation was different from that of the control genotype in the same direction (up- or down-regulated) in at least two transgenic lines either by *P*-value (*P* < 0.05) or by log fold change (>1.0 or < -1.0). Distribution of DEGs within the three analyzed *SITBP*-knock-down lines is shown in Supplementary Fig. S5. Functional categorization of DEGs was performed using the MapMan software (Thimm et al. 2004).

### Starch quantification

Starch content was spectrophotometrically determined in T<sub>0</sub> generation transgenic lines (Dominguez et al. 2013).

### Polar metabolite profiles

Extraction, derivatization, standard addition and sample injection for GC-MS were performed as previously described (Lisec et al. 2006, Osorio et al. 2012). Identification and quantification of the compounds were performed with TagFinder 4.0 software, and the mass spectra were cross-referenced with those in the Golm Metabolome Database (Kopka et al. 2005, Schauer et al. 2005). Three to six biological replicates were used for this analysis.

### Data analyses

Differences in parameters were analyzed using Infostat software version 2011 (<http://www.infostat.com.ar>). When the data set showed homoscedasticity, ANOVA-Tukey test (*P* < 0.05) was performed to compare transgenic lines against the control genotype. In the absence of homoscedasticity, a non-parametric comparison was performed by applying the Kruskal–Wallis test (*P* < 0.05). All values represent the mean of at least three biological replicates. A parameter was considered to be affected by *SITBP* silencing if at least 50% of the tested *SITBP*-knockdown lines differed significantly from the wild-type genotype in the same direction.

### Supplementary Data

Supplementary data are available at PCP online.

### Funding

This work was supported by Fundação de Amparo à Pesquisa do Estado de São Paulo (Brazil; FAPESP, 2010-50535-0); Conselho Nacional de Desenvolvimento Científico e Tecnológico (CNPq, Brazil); Coordenação de Aperfeiçoamento de Pessoal de Nível Superior (CAPES, Brazil); Universidade de São Paulo (USP, Brazil); Instituto Nacional de Tecnología Agropecuaria (INTA, Argentina); Agencia Nacional de Promoción Científica y Tecnológica; Consejo Nacional de Investigaciones Científicas y Técnicas (CONICET, Argentina); Facultad de Agronomía de la Universidad de Buenos Aires (FAUBA, Argentina); European Union Horizon 2020 Research and Innovation Programme (Grant Agreement Number 679796); Fondo de Financiamiento de Centros de Investigación em Áreas Prioritárias (FONDAP, 50 15090007,

Chile); Fondo Nacional de Desarrollo Científico y Tecnológico (FONDECYT, 11160899, Chile); The Novo Nordisk Foundation (Biotechnology-based Synthesis and Production Research); The Villum Foundation (PLANET Project); the Danish Agency for Science, Technology and Innovation (Danish–Brazilian Network for Plant Glycoscience); and the MINCYT-ECOS program 55 (Argentina–France). L.B., B.S.L., F.G. and J.A. were recipients of FAPESP fellowships. L.B., M.R., and D.D. were funded by a fellowship from CNPq. L.B., R.A. and F.C. are members of the Argentine Council of Science and Technology (CONICET).

### Acknowledgments

Imaging was performed at the Bordeaux Imaging Center, a member of the national infrastructure France Biolmaging. The help of B. Batailler in this work is acknowledged.

### Disclosures

The authors declare no conflicts of interest.

### References

- Almeida, J., da Silva Azevedo, M., Spicher, L., Glauser, G., Vom Dorp, K., Guyer, L., et al. (2016) Down-regulation of tomato PHYTOL KINASE strongly impairs tocopherol biosynthesis and affects prenyllipid metabolism in an organ-specific manner. *J. Exp. Bot.* 67: 919–934.
- Almeida, J., Quadrana, L., Asís, R., Setta, N., de Godoy, F. and Bermúdez, L. (2011) Genetic dissection of vitamin E biosynthesis in tomato. *J. Exp. Bot.* 62: 3781–3798.
- Anantharaman, V. and Aravind, L. (2002) The GOLD domain, a novel protein module involved in Golgi function and secretion. *Genome Biol.* 3: research0023.
- Andrews, P.K., Fahy, D.A. and Foyer, C.H. (2004) Relationships between fruit exocarp antioxidants in the tomato (*Lycopersicon esculentum*) high pigment-1 mutant during development. *Physiol. Plant.* 120: 519–528.
- Auldridge, M.E., Block, A., Vogel, J.T., Dabney-Smith, C., Mila, I., Bouzayen, M., et al. (2006) Characterization of three members of the Arabidopsis carotenoid cleavage dioxygenase family demonstrates the divergent roles of this multifunctional enzyme family. *Plant J.* 45: 982–993.
- Austin, J.R. (2006) Plastoglobules are lipoprotein subcompartments of the chloroplast that are permanently coupled to thylakoid membranes and contain biosynthetic enzymes. *Plant Cell Online* 18: 1693–1703.
- Bankaitis, V.A., Mousley, C.J. and Schaaf, G. (2010) The Sec14-superfamily and mechanisms for crosstalk between lipid metabolism and lipid signaling. *Trends Biochem. Sci.* 35: 150–160.
- Castro, E., de Sigris, C.J.A., Gattiker, A., Bulliard, V., Langendijk-Genevaux, P.S., Gasteiger, E., et al. (2006) ScanProsite: detection of PROSITE signature matches and ProRule-associated functional and structural residues in proteins. *Nucleic Acids Res.* 34: W362–W365.
- de Campos, M.K.F. and Schaaf, G. (2017) The regulation of cell polarity by lipid transfer proteins of the SEC14 family. *Curr. Opin. Plant Biol.* 40: 158–168.
- Deranieh, R.M., Joshi, A.S. and Greenberg, M.L. (2013) Thin-layer chromatography of phospholipids. *Methods Mol. Biol.* 1033: 21–27.
- Dereeper, A., Guignon, V., Blanc, G., Audic, S., Buffet, S., Chevenet, F., et al. (2008) Phylogeny.fr: robust phylogenetic analysis for the non-specialist. *Nucleic Acids Res.* 36: W465–W469.

- Dominguez, P.G., Frankel, N., Mazuch, J., Balbo, I., Iusem, N., Fernie, A.R., *et al.* (2013) ASR1 mediates glucose–hormone cross talk by affecting sugar trafficking in tobacco plants. *Plant Physiol.* 161: 1486–1500.
- Dorp, K., Vom Hözl, G., Plohmann, C., Eisenhut, M., Abraham, M., Weber, A.P.M., *et al.* (2015) Remobilization of phytol from chlorophyll degradation is essential for tocopherol synthesis and growth of Arabidopsis. *Plant Cell* 27: 2846–2859.
- Dudareva, N., Martin, D., Kish, C.M., Kolosova, N., Gorenstein, N., Fäldt, J., *et al.* (2003) (E)- $\beta$ -Ocimene and myrcene synthase genes of floral scent biosynthesis in snapdragon: function and expression of three terpene synthase genes of a new terpene synthase subfamily. *Plant Cell* 15: 1227–1241.
- Emanuelsson, O., Nielsen, H. and von Heijne, G. (1999) ChloroP, a neural network-based method for predicting chloroplast transit peptides and their cleavage sites. *Protein Sci.* 8: 978–984.
- Folch, J. (1987) A simple method for the isolation and purification of total lipids from animal tissues. *J. Biol. Chem.* 55: 999–1033.
- Foyer, C.H. and Shigeoka, S. (2011) Understanding oxidative stress and antioxidant functions to enhance photosynthesis. *Plant Physiol.* 155: 93–100.
- Giovannoni, J., Nguyen, C., Ampofo, B., Zhong, S. and Fei, Z. (2017) The epigenome and transcriptional dynamics of fruit ripening. *Annu. Rev. Plant Biol.* 68: 61–84.
- Godoy, F., de Bermudez, L., Lira, B.S., de Souza, A.P., Elbl, P., Demarco, D., *et al.* (2013) Galacturonosyltransferase 4 silencing alters pectin composition and carbon partitioning in tomato. *J. Exp. Bot.* 64: 2449–2466.
- Gonzalez-Jorge, S., Ha, S.-H., Magallanes-Lundback, M., Gilliland, L.U., Zhou, A., Lipka, A.E., *et al.* (2013) CAROTENOID CLEAVAGE DIOXYGENASE4 is a negative regulator of  $\beta$ -carotene content in Arabidopsis seeds. *Plant Cell* 25: 4812–4826.
- Guindon, S., Dufayard, J.-F., Lefort, V., Anisimova, M., Hordijk, W. and Gascuel, O. (2010) New algorithms and methods to estimate maximum-likelihood phylogenies: assessing the performance of PhyML 3.0. *Syst. Biol.* 59: 307–321.
- Havaux, M., Dall’Osto, L. and Bassi, R. (2007) Zeaxanthin has enhanced antioxidant capacity with respect to all other xanthophylls in Arabidopsis leaves and functions independent of binding to PSII antennae. *Plant Physiol.* 145: 1506–1520.
- Havaux, M., Eymery, F., Porfirova, S., Rey, P. and Dörmann, P. (2005) Vitamin E protects against photoinhibition and photooxidative stress in Arabidopsis thaliana. *Plant Cell* 17: 3451–3469.
- Heath, R.L. and Packer, L. (1968) Photoperoxidation in isolated chloroplasts: I. Kinetics and stoichiometry of fatty acid peroxidation. *Arch. Biochem. Biophys.* 125: 189–198.
- Heredia, A., Peinado, I., Barrera, C. and Grau, A.A. (2009) Influence of process variables on colour changes, carotenoids retention and cellular tissue alteration of cherry tomato during osmotic dehydration. *J. Food Compos. Anal.* 22: 285–294.
- Hölscher, C., Meyer, T. and Von Schaeuwen, A. (2014) Dual-targeting of arabidopsis 6-phosphogluconolactonase 3 (PGL3) to chloroplasts and peroxisomes involves interaction with Trx m2 in the cytosol. *Mol. Plant* 7: 252–255.
- Jones, P., Binns, D., Chang, H.-Y., Fraser, M., Li, W., McAnulla, C., *et al.* (2014) InterProScan 5: genome-scale protein function classification. *Bioinformatics* 30: 1236–1240.
- Juguelin, H., Heape, A., Boiron, F. and Cassagne, C. (1986) A quantitative developmental study of neutral lipids during myelinogenesis in the peripheral nervous system of normal and trembler mice. *Dev. Brain Res.* 25: 249–252.
- Karimi, M., Inzé, D. and Depicker, A. (2002) GATEWAY<sup>TM</sup> vectors for Agrobacterium-mediated plant transformation. *Trends Plant Sci.* 7: 193–195.
- Keim, V., Manzano, D., Fernández, F.J., Closa, M., Andrade, P., Caudepón, D., *et al.* (2012) Characterization of Arabidopsis FPS isozymes and FPS gene expression analysis provide insight into the biosynthesis of isoprenoid precursors in seeds. *PLoS One* 7: e49109.
- Kono, N., Ohto, U., Hiramatsu, T., Urabe, M., Uchida, Y., Satow, Y., *et al.* (2013) Impaired  $\alpha$ -TTP–PIPs interaction underlies familial vitamin E deficiency. *Science* 340: 1106–1110.
- Kopka, J., Schauer, N., Krueger, S., Birkemeyer, C., Usadel, B., Bergmüller, E., *et al.* (2005) GMD@CSB.DB: the Golm metabolome database. *Bioinformatics* 21: 1635–1638.
- Krieger-Liszak, A. and Trebst, A. (2006) Tocopherol is the scavenger of singlet oxygen produced by the triplet states of chlorophyll in the PSII reaction centre. *J. Exp. Bot.* 57: 1677–1684.
- Li-Beisson, Y., Shorosh, B., Beisson, F., Andersson, M.X., Arondel, V., Bates, P.D., *et al.* (2010) Acyl-lipid metabolism. *Arabidopsis Book* 8: e0133.
- Lichtenthaler, H.K. (1987) Chlorophylls and carotenoids: pigments of photosynthetic biomembranes. *Methods Enzymol.* 148: 350–382.
- Lippold, F., Dorp, K., Vom Abraham, M., Hözl, G., Wewer, V., Yilmaz, J.L., *et al.* (2012) Fatty acid phytol ester synthesis in chloroplasts of Arabidopsis. *Plant Cell* 24: 2001–2014.
- Lira, B.S., Gramegna, G., Trench, B., Alves, F.R.R., Silva, É.M., Silva, G.F.F., *et al.* (2017) Manipulation of a senescence-associated gene improves fleshy fruit yield. *Plant Physiol.* 175: 77–91.
- Lisec, J., Schauer, N., Kopka, J., Willmitzer, L. and Fernie, A.R. (2006) Gas chromatography mass spectrometry-based metabolite profiling in plants. *Nat. Protoc.* 1: 387–396.
- Löbbecke, L. and Cevc, G. (1995) Effects of short-chain alcohols on the phase behavior and interdigitation of phosphatidylcholine bilayer membranes. *Biochim. Biophys. Acta Biomembr.* 1237: 59–69.
- Lohse, M., Nunes-Nesi, A., Krüger, P., Nagel, A., Hannemann, J., Giorgi, F.M., *et al.* (2010) Robin: an intuitive wizard application for R-based expression microarray quality assessment and analysis. *Plant Physiol.* 153: 642–651.
- Maeda, H., Sage, T.L., Isaac, G., Welti, R. and DellaPenna, D. (2008) Tocopherols modulate extraplastidic polyunsaturated fatty acid metabolism in Arabidopsis at low temperature. *Plant Cell* 20: 452–470.
- Mehrshahi, P., Johnny, C. and DellaPenna, D. (2014) Redefining the metabolic continuity of chloroplasts and ER. *Trends Plant Sci.* 19: 501–507.
- Mehrshahi, P., Stefano, G., Andaloro, J.M., Brandizzi, F., Froehlich, J.E. and DellaPenna, D. (2013) Transorganellar complementation redefines the biochemical continuity of endoplasmic reticulum and chloroplasts. *Proc. Natl. Acad. Sci. USA* 110: 12126–12131.
- Meier, R., Tomizaki, T., Schulze-Briese, C., Baumann, U. and Stocker, A. (2003) The molecular basis of vitamin E retention: structure of human  $\alpha$ -tocopherol transfer protein. *J. Mol. Biol.* 331: 725–734.
- Miller, M.B., Vishwanatha, K.S., Mains, R.E. and Eipper, B.A. (2015) An N-terminal amphipathic helix binds phosphoinositides and enhances kaliRIN Sec14 domain-mediated membrane interactions. *J. Biol. Chem.* 290: 13541–13555.
- Min, K.C., Kovall, R.A. and Hendrickson, W.A. (2003) Crystal structure of human  $\alpha$ -tocopherol transfer protein bound to its ligand: implications for ataxia with vitamin E deficiency. *Proc. Natl. Acad. Sci. USA* 100: 14713–14718.
- Miret, J.A. and Munné-Bosch, S. (2015) Redox signaling and stress tolerance in plants: a focus on vitamin E. *Ann. N.Y. Acad. Sci.* 1340: 29–38.
- Nacir, H. and Bréhélin, C. (2013) When proteomics reveals unsuspected roles: the plastoglobule example. *Front. Plant Sci.* 4: 114.
- Nava, P., Cecchini, M., Chirico, S., Gordon, H., Morley, S., Manor, D., *et al.* (2006) Preparation of fluorescent tocopherols for use in protein binding and localization with the alpha-tocopherol transfer protein. *Bioorg. Med. Chem.* 14: 3721–3736.
- Nunes-Nesi, A., Carrari, F., Lytovchenko, A., Smith, A.M.O., Loureiro, M.E., Ratcliffe, R.G., *et al.* (2005) Enhanced photosynthetic performance and growth as a consequence of decreasing mitochondrial malate dehydrogenase activity in transgenic tomato plants. *Plant Physiol.* 137: 611–622.
- Osorio, S., Do, P.T. and Fernie, A.R. (2012) Plant metabolomics. *Methods Mol. Biol.* 860: 101–109.

- Padham, A.K., Hopkins, M.T., Wang, T.-W., McNamara, L.M., Lo, M., Richardson, L.G.L., et al. (2007) Characterization of a plastid triacylglycerol lipase from *Arabidopsis*. *Plant Physiol.* 143: 1372–1384.
- Panagabko, C., Morley, S., Hernandez, M., Cassolato, P., Gordon, H., Parsons, R., et al. (2003) Ligand specificity in the CRAL–TRIO protein family. *Biochemistry* 42: 6467–6474.
- Pellaud, S. and Mène Saffrané, L. (2017) Metabolic origins and transport of vitamin E biosynthetic precursors. *Front. Plant Sci.* 8: 1959.
- Peterman, T.K. (2004) Patellin1, a novel Sec14-like protein, localizes to the cell plate and binds phosphoinositides. *Plant Physiol.* 136: 3080–3094.
- Peterman, T.K., Ohol, Y.M., McReynolds, L.J., Luna, E.J., Sciences, B., College, W., et al. (2004) Patellin1, a novel Sec14-like protein, localizes to the cell plate and binds phosphoinositides 1. *Plant Physiol.* 136: 3080–3015.
- Peterman, T.K., Sequeira, A.S., Samia, J.A. and Lunde, E.E. (2006) Molecular cloning and characterization of patellin1, a novel sec14-related protein, from zucchini (*Cucurbita pepo*). *J. Plant Physiol.* 163: 1150–1158.
- Pfaffl, M.W., Horgan, G.W. and Dempfle, L. (2002) Relative expression software tool (REST) for group-wise comparison and statistical analysis of relative expression results in real-time PCR. *Nucleic Acids Res.* 30: 36.
- Quadrana, L., Almeida, J., Asís, R., Duffy, T., Dominguez, P.G., Bermúdez, L., et al. (2014) Natural occurring epialleles determine vitamin E accumulation in tomato fruits. *Nat. Commun.* 5: 4027.
- Quadrana, L., Almeida, J., Otaiza, S.N., Duffy, T., Da Silva, J.V.C., de Godoy, F., et al. (2013) Transcriptional regulation of tocopherol biosynthesis in tomato. *Plant Mol. Biol.* 81: 309–325.
- Saito, K., Tautz, L. and Mustelin, T. (2007) The lipid-binding SEC14 domain. *Biochim. Biophys. Acta* 1771: 719–726.
- Schaaf, G., Ortlund, E.A., Tyeryar, K.R., Mousley, C.J., Ile, K.E., Garrett, T.A., et al. (2008) Functional anatomy of phospholipid binding and regulation of phosphoinositide homeostasis by proteins of the sec14 superfamily. *Mol. Cell* 29: 191–206.
- Schauer, N., Semel, Y., Roessner, U., Gur, A., Balbo, I., Carrari, F., et al. (2006) Comprehensive metabolic profiling and phenotyping of interspecific introgression lines for tomato improvement. *Nat. Biotechnol.* 24: 447–454.
- Schauer, N., Zamir, D. and Fernie, A.R. (2005) Metabolic profiling of leaves and fruit of wild species tomato: a survey of the *Solanum lycopersicum* complex. *J. Exp. Bot.* 56: 297–307.
- Sikkema, J., Bont, J.A. and de Poolman, B. (1995) Mechanisms of membrane toxicity of hydrocarbons. *Microbiol. Rev.* 59: 201–222.
- Simkin, A.J., Underwood, B.A., Auldrige, M., Loucas, H.M., Shibuya, K., Schmelz, E., et al. (2004) Circadian regulation of the PhCCD1 carotenoid cleavage dioxygenase controls emission of  $\beta$ -ionone, a fragrance volatile of petunia flowers 1. *Plant Physiol.* 136: 3504–3514.
- Smyth, G.K. (2004) Linear models and empirical bayes methods for assessing differential expression in microarray experiments. *Stat. Appl. Genet. Mol. Biol.* 3: 1–25.
- Smyth, G.K. and Speed, T. (2003) Normalization of cDNA microarray data. *Methods* 31: 265–273.
- Song, W., Maeda, H. and DellaPenna, D. (2010) Mutations of the ER to plastid lipid transporters TGD1, 2, 3 and 4 and the ER oleate desaturase FAD2 suppress the low temperature-induced phenotype of *Arabidopsis* tocopherol-deficient mutant *vte2*. *Plant J.* 62: 1004–1018.
- Spicher, L., Almeida, J., Gutbrod, K., Pipitone, R., Dürmann, P., Glauser, G., et al. (2017) Essential role for phytol kinase and tocopherol in tolerance to combined light and temperature stress in tomato. *J. Exp. Bot.* 68: 5845–5856.
- Spicher, L. and Kessler, F. (2015) Unexpected roles of plastoglobules (plastid lipid droplets) in vitamin K and E metabolism. *Curr. Opin. Plant Biol.* 25: 123–129.
- Stevenson, J.M., Perera, I.Y., Heilmann, I., Persson, S. and Boss, W.F. (2000) Inositol signaling and plant growth. *Trends Plant Sci.* 5: 252–258.
- Stocker, A. and Baumann, U. (2003) Supernatant protein factor in complex with RRR- $\alpha$ -tocopherylquinone: a link between oxidized Vitamin E and cholesterol biosynthesis. *J. Mol. Biol.* 332: 759–765.
- Suzuki, T., Matsushima, C., Nishimura, S., Higashiyama, T., Sasabe, M. and Machida, Y. (2016) Identification of phosphoinositide-binding protein PATELLIN2 as a substrate of *Arabidopsis* MPK4 MAP kinase during septum formation in cytokinesis. *Plant Cell Physiol.* 57: 1744–1755.
- Tamura, K., Stecher, G., Peterson, D., Filipowski, A. and Kumar, S. (2013) MEGA6: molecular evolutionary genetics analysis version 6.0. *Mol. Biol. Evol.* 30: 2725–2729.
- Tanksley, S.D. (2004) The genetic, developmental, and molecular bases of fruit size and shape variation in tomato. *Nature* 16: 181–189.
- Thimm, O., Bläsing, O., Gibon, Y., Nagel, A., Meyer, S., Krüger, P., et al. (2004) MAPMAN: a user-driven tool to display genomics data sets onto diagrams of metabolic pathways and other biological processes. *Plant J.* 37: 914–939.
- Valentin, H.E. (2006) The *Arabidopsis* vitamin E pathway gene5-1 mutant reveals a critical role for phytol kinase in seed tocopherol biosynthesis. *Plant Cell* 18: 212–224.
- Vidi, P.-A., Kanwischer, M., Baginsky, S., Austin, J.R., Csucs, G., Dörmann, P., et al. (2006) Tocopherol cyclase (VTE1) localization and vitamin E accumulation in chloroplast plastoglobule lipoprotein particles. *J. Biol. Chem.* 281: 11225–11234.
- Wang, M., Toda, K. and Maeda, H.A. (2016) Biochemical properties and subcellular localization of tyrosine aminotransferases in *Arabidopsis thaliana*. *Phytochem* 132: 16–25.
- Yang, Y.H., Dudoit, S., Luu, P., Lin, D.M., Peng, V., Ngai, J., et al. (2002) Normalization for cDNA microarray data: a robust composite method addressing single and multiple slide systematic variation. *Nucleic Acids Res.* 30: e15–e15.
- Yang, W., Wang, G., Li, J., Bates, P.D., Wang, X. and Allen, D.K. (2017) Phospholipase D $\zeta$  enhances diacylglycerol flux into triacylglycerol. *Plant Physiol.* 174: 110–123.